

DESY 05-237
Edinburgh 2005/18
Liverpool LTH 672
January 2006

Estimating the Unquenched Strange Quark Mass from the Lattice Axial Ward Identity

M. Göckeler¹, R. Horsley², A. C. Irving³,
D. Pleiter⁴, P. E. L. Rakow³, G. Schierholz^{4,5},
H. Stüben⁶ and J. M. Zanotti²

– QCDSF-UKQCD Collaboration –

¹ Institut für Theoretische Physik, Universität Regensburg,
D-93040 Regensburg, Germany

² School of Physics, University of Edinburgh,
Edinburgh EH9 3JZ, UK

³ Department of Mathematical Sciences, University of Liverpool,
Liverpool L69 3BX, UK

⁴ John von Neumann-Institut für Computing NIC,
Deutsches Elektronen-Synchrotron DESY,
D-15738 Zeuthen, Germany

⁵ Deutsches Elektronen-Synchrotron DESY,
D-22603 Hamburg, Germany

⁶ Konrad-Zuse-Zentrum für Informationstechnik Berlin,
D-14195 Berlin, Germany

Abstract

We present a determination of the strange quark mass for two flavours ($n_f = 2$) of light dynamical quarks using the axial Ward identity. The calculations are performed on the lattice using $O(a)$ improved Wilson fermions and include a fully non-perturbative determination of the renormalisation constant. In the continuum limit we find $m_s^{\overline{MS}}(2 \text{ GeV}) = 111(6)(4)(6) \text{ MeV}$, using the force scale $r_0 = 0.467 \text{ fm}$, where the first error is statistical, the second and third are systematic due to the fit and scale uncertainties respectively. Results are also presented for the light quark mass and the chiral condensate. The corresponding results are also given for $r_0 = 0.5 \text{ fm}$.

1 Introduction

Lattice methods allow, in principle, an ‘ab initio’ calculation of the fundamental parameters of QCD, among them the quark masses. Quarks are not asymptotic states of QCD and so quark masses need to be defined by a renormalisation procedure,

$$m_q^{\mathcal{S}}(M) = Z_m^{\mathcal{S}}(M)m_q^{\text{bare}}, \quad (1)$$

by giving the scheme \mathcal{S} and scale M .

To convert the lattice results to continuum numbers, one needs control over the discretisation errors and the matching relations between the lattice scheme and the continuum renormalisation scheme \mathcal{S} . Discretisation errors can be kept small and manageable by employing an improved fermion action. But, still, the lattice numbers may show considerable cut-off dependence at present couplings, which requires that the calculations are done over a range of sufficiently small lattice spacings a , discretisation errors then being removed by an extrapolation to $a = 0$. The perturbative relations between renormalised quantities in the continuum and the bare lattice results are in almost all cases known to one-loop order only. Data show (for example [1]) that $O(\alpha_s^2)$ corrections can be large, $O(10 - 20\%)$ at spacings $a \approx 0.1$ fm, which makes a non-perturbative calculation of the renormalisation constants indispensable.

Many calculations of the strange quark mass, both with $n_f = 2$ [2, 3, 4] and $n_f = 2+1$ [5, 6, 7, 8] flavours of sea quarks, employed perturbative renormalisation of the bare quark mass and were restricted to lattice spacings $a \gtrsim 0.1$ fm. (Recent $n_f = 2 + 1$ results [7], have finer lattice spacings.) These authors quote strange quark masses of $O(80)$ MeV, lying 15 – 30% below the corresponding quenched results [9, 10].

In [11] we have presented an entirely non-perturbative (NP) calculation of the light quark masses based on the vector Ward identity (VWI), using non-perturbatively $O(a)$ improved Wilson fermions with $n_f = 2$ flavours of dynamical quarks. The calculation was done at four different lattice spacings $0.065 \lesssim a \lesssim 0.09$ fm, which allowed us to perform a continuum extrapolation. We found a strange quark mass of $m_s^{\overline{\text{MS}}}(2 \text{ GeV}) = 119(5)(8)$ MeV. A highlight and essential ingredient of the calculation was that we were able to compute the flavour singlet mass renormalisation constant, which is needed in the VWI approach.

This result has been complemented recently by further studies in [12, 13] which also used NP determinations of the renormalisation constant.

In this paper we present an independent calculation of the strange quark mass using the axial vector Ward identity (AWI), again for $n_f = 2$ flavours of improved Wilson fermions. The AWI involves only non-singlet quantities and thus provides an important test of our previous calculation.

The paper is organised as follows. As we shall be considering not only the $\overline{\text{MS}}$

scheme, but also the RI'-MOM scheme (which is more convenient for a lattice calculation) we first discuss in section 2 renormalisation group invariants (RGIs), taking the quark mass as an example, and how to convert to them. We also collect together relevant formulae for the $\overline{\text{MS}}$ scheme. Also discussed is the unit and scale we shall use – the r_0 -force scale – and thus the relevant conversion factor to physical units. In section 3 we compile some results from leading order (LO) and next to leading order (NLO) chiral perturbation theory (χ PT) and re-write them in a form suitable for our calculation. Section 4 describes some lattice details relevant for $O(a)$ improved fermions. This is followed in section 5 by the non-perturbative computation of the renormalisation constant. Relevant results for the RI'-MOM scheme are given, both for the the lattice computation of $Z_m^{\text{RI}'\text{-MOM}}$ and for the conversion to the RGI form. The section is concluded with a comparison of this result with the results obtained by other approaches (principally the tadpole improved (TI) perturbation theory method). In section 6 results are given for the strange quark mass, first at finite lattice spacing, and then the continuum extrapolation is performed to give our final answer. Finally in the last section, section 7, we compare our AWI result with the previously obtained VWI result and also with other recent mass determinations. In the appendix, tables of our raw data results for the quark mass are given.

2 Renormalisation Group Invariants

The ‘running’ of the renormalised quark mass as the scale M is changed is controlled by the β and γ functions in the renormalisation group equation, defined by

$$\beta^{\mathcal{S}}(g^{\mathcal{S}}(M)) \equiv \left. \frac{\partial g^{\mathcal{S}}(M)}{\partial \log M} \right|_{\text{bare}}, \quad (2)$$

$$\gamma_m^{\mathcal{S}}(g^{\mathcal{S}}(M)) \equiv \left. \frac{\partial \log Z_m^{\mathcal{S}}(M)}{\partial \log M} \right|_{\text{bare}}, \quad (3)$$

where the bare parameters are held constant. These functions are given perturbatively as power series expansions in the coupling constant,

$$\begin{aligned} \beta^{\mathcal{S}}(g) &= -b_0 g^3 - b_1 g^5 - b_2^{\mathcal{S}} g^7 - b_3^{\mathcal{S}} g^9 - \dots, \\ \gamma_m^{\mathcal{S}}(g) &= d_{m0} g^2 + d_{m1}^{\mathcal{S}} g^4 + d_{m2}^{\mathcal{S}} g^6 + d_{m3}^{\mathcal{S}} g^8 + \dots \end{aligned} \quad (4)$$

The first two coefficients of the β -function and first coefficient of the γ_m function are scheme independent,

$$b_0 = \frac{1}{(4\pi)^2} \left(11 - \frac{2}{3} n_f \right), \quad b_1 = \frac{1}{(4\pi)^4} \left(102 - \frac{38}{3} n_f \right). \quad (5)$$

and

$$d_{m0} = -\frac{8}{(4\pi)^2}, \quad (6)$$

while all others depend on the scheme chosen.

We may immediately integrate eq. (2) to obtain

$$\frac{M}{\Lambda^S} = [b_0 g^S(M)^2]^{\frac{b_1}{2b_0^2}} \exp\left[\frac{1}{2b_0 g^S(M)^2}\right] \exp\left\{\int_0^{g^S(M)} d\xi \left[\frac{1}{\beta^S(\xi)} + \frac{1}{b_0 \xi^3} - \frac{b_1}{b_0^2 \xi}\right]\right\}. \quad (7)$$

The renormalisation group invariant quark mass¹ is defined from the renormalised quark mass as

$$m_q^{\text{RCI}} \equiv \Delta Z_m^S(M) m^S(M) = \Delta Z_m^S(M) Z_m^S(M) m_q^{\text{bare}} \equiv Z_m^{\text{RCI}} m_q^{\text{bare}}, \quad (8)$$

where

$$[\Delta Z_m^S(M)]^{-1} = [2b_0 g^S(M)^2]^{-\frac{d_{m0}}{2b_0}} \exp\left\{\int_0^{g^S(M)} d\xi \left[\frac{\gamma_m^S(\xi)}{\beta^S(\xi)} + \frac{d_{m0}}{b_0 \xi}\right]\right\}, \quad (9)$$

and so the integration constant upon integrating eq. (2) is given by Λ^S , and similarly from eq. (3) the integration constant is m_q^{RCI} . Λ^S and m_q^{RCI} are thus independent of the scale. (Note that although the functional form of $\Delta Z_m^S(M)$ is fixed, the absolute value is not; conventions vary for its definition.) Also for a scheme change $\mathcal{S} \rightarrow \mathcal{S}'$ (it is now sufficient to take them at the same scale) given by

$$g^{\mathcal{S}'} = G(g^{\mathcal{S}}) = g^{\mathcal{S}}(1 + \frac{1}{2}t_1(g^{\mathcal{S}})^2 + \dots), \quad (10)$$

then m_q^{RCI} remains invariant, while Λ changes as $\Lambda^{\mathcal{S}'} = \Lambda^{\mathcal{S}} \exp(t_1/(2b_0))$. Note also that analytic expressions for the integrals in eq. (8) or eq. (9) can be found for low orders, for example to two loops we have

$$\Delta Z_m^S(M) = [2b_0 (g^S(M))^2]^{\frac{d_{m0}}{2b_0}} \left[1 + \frac{b_1}{b_0} (g^S(M))^2\right]^{\frac{b_0 d_{m1}^S - b_1 d_{m0}}{2b_0 b_1}}. \quad (11)$$

Thus we have a convenient splitting of the problem into two parts: a number, m_q^{RCI} , which involves a non-perturbative computation, and is the goal of this paper and, if desired, an evaluation of ΔZ_m^S which allows the running quark mass to be given in a renormalisation scheme \mathcal{S} .

In the remainder of this section we discuss the evaluation of ΔZ_m^S in the $\overline{\text{MS}}$ -scheme, which is conventionally used, and for which four coefficients in the

¹Analogous definitions hold for other quantities which depend on the scheme and scale chosen.

perturbative expansion are known. For the β function we have [14, 15, 16],

$$\begin{aligned} b_2^{\overline{MS}} &= \frac{1}{(4\pi)^6} \left[\frac{2857}{2} - \frac{5033}{18}n_f + \frac{325}{54}n_f^2 \right], \\ b_3^{\overline{MS}} &= \frac{1}{(4\pi)^8} \left[\frac{149753}{6} + 3564\zeta_3 - \left(\frac{1078361}{162} + \frac{6508}{27}\zeta_3 \right)n_f \right. \\ &\quad \left. + \left(\frac{50065}{162} + \frac{6472}{81}\zeta_3 \right)n_f^2 + \frac{1093}{729}n_f^3 \right], \end{aligned} \quad (12)$$

and for the γ_m function [17, 18],

$$\begin{aligned} d_{m1}^{\overline{MS}} &= -\frac{1}{(4\pi)^4} \left[\frac{404}{3} - \frac{40}{9}n_f \right], \\ d_{m2}^{\overline{MS}} &= -\frac{1}{(4\pi)^6} \left[2498 - \left(\frac{4432}{27} + \frac{320}{3}\zeta_3 \right)n_f - \frac{280}{81}n_f^2 \right], \\ d_{m3}^{\overline{MS}} &= -\frac{1}{(4\pi)^8} \left[\frac{4603055}{81} + \frac{271360}{27}\zeta_3 - 17600\zeta_5 \right. \\ &\quad \left. - \left(\frac{183446}{27} + \frac{68384}{9}\zeta_3 - 1760\zeta_4 - \frac{36800}{9}\zeta_5 \right)n_f \right. \\ &\quad \left. + \left(\frac{10484}{243} + \frac{1600}{9}\zeta_3 - \frac{320}{3}\zeta_4 \right)n_f^2 - \left(\frac{664}{243} - \frac{128}{27}\zeta_3 \right)n_f^3 \right], \end{aligned} \quad (13)$$

with $\zeta_3 = 1.20206\dots$, $\zeta_4 = 1.08232\dots$ and $\zeta_5 = 1.03693\dots$, ζ being the Riemann zeta function.

This scheme is a manifestly perturbative scheme and so should be used at a high enough scale $M \equiv \mu$ so that perturbation theory is reliable. Computing $[\Delta Z_m^{\overline{MS}}(\mu)]^{-1}$ involves first solving eq. (7) for $g^{\overline{MS}}$ (as a function of $\mu/\Lambda^{\overline{MS}}$) and then evaluating eq. (9). Practically we expand the β and γ functions to the appropriate order and then numerically evaluate the integrals. The final results are given in Fig. 1.

Conventionally light quark masses are defined at a scale of $\mu = 2 \text{ GeV}$, which means giving a value for $\Lambda^{\overline{MS}}$ in MeV. We set the scale here by using the ‘force scale’ r_0 , which means first changing from the $\Lambda^{\overline{MS}}$ unit to the r_0 unit. From [19] (see also [20]), we use the value

$$r_0 \Lambda^{\overline{MS}} = 0.617(40)(21). \quad (14)$$

The r_0 scale in MeV still needs to be set. A popular choice is

$$r_0 = 0.5 \text{ fm} \equiv 1/(394.6 \text{ MeV}), \quad (15)$$

which is useful when making comparisons with other results for the quark mass. Alternatively from a fit to the dimensionless nucleon mass $r_0 m_N$ using results obtained by the CP-PACS, JLQCD and QCDSF-UKQCD collaborations, following [21] we found a scale of

$$r_0 = 0.467(33) \text{ fm} \equiv 1/(422.5(29.9) \text{ MeV}). \quad (16)$$

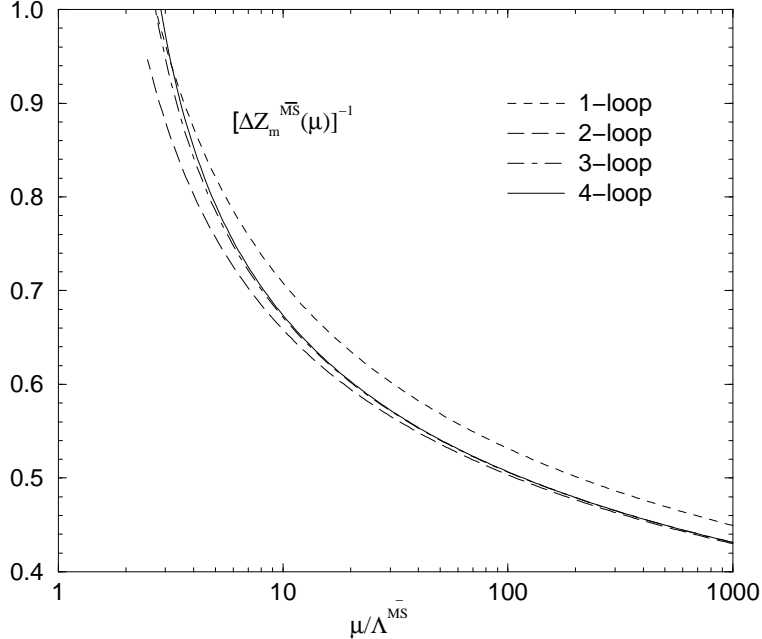


Figure 1: One-, two-, three- and four-loop results for $[\Delta Z_m^{\overline{MS}}(\mu)]^{-1}$ in units of $\Lambda^{\overline{MS}}$.

r_0	one-loop	two-loop	three-loop	four-loop
0.5 fm	0.735(11)	0.682(10)	0.698(11)	0.700(11)
0.467 fm	0.745(12)	0.690(10)	0.707(12)	0.711(12)

Table 1: Values of $[\Delta Z_m^{\overline{MS}}(\mu)]^{-1}$ at $\mu = 2 \text{ GeV}$. The errors are a reflection of the errors in eq. (14).

Similar results were obtained in [22, 23]. The 0.033 fm error in the $r_0 = 0.467 \text{ fm}$ estimate is roughly equal to the difference between the two r_0 values. As these different r_0 values give an idea of the uncertainties involved in setting the scale we shall derive results using both values of r_0 and regard this as giving an estimate of a possible scale systematic error. The different values of r_0 in eqs. (15), (16) give $\Lambda^{\overline{MS}} = 243(16)(8) \text{ MeV}$ and $261(17)(9) \text{ MeV}$ respectively.

Results for $[\Delta Z_m^{\overline{MS}}]^{-1}$ at $\mu = 2 \text{ GeV}$ are given in Table 1. At $\mu = 2 \text{ GeV}$ we have $\mu/\Lambda^{\overline{MS}} \approx 8$, and it seems that already at this value we have a rapidly converging series in loop orders. Indeed, only going from one loop to two loops gives a significant change in $[\Delta Z_m^{\overline{MS}}]^{-1}$ of order 8%. From two loops to three loops we have about 2%. The difference between the three-loop and four-loop results is $O(\frac{1}{2}\%)$. So if we are given m_q^{RGI} , and we wish to find the quark mass in the \overline{MS} scheme at a certain scale, we shall use the four-loop result from eq. (9) as shown in Fig. 1.

3 Chiral Perturbation Theory

Chiral perturbation theory (χ PT) gives the LO and NLO result² [25, 26] for n_f degenerate sea quarks of

$$\left(\frac{m_{ps}^{AB}}{4\pi f_0}\right)^2 = \chi_{AB} \left[1 + \chi_S n_f (2\alpha_6 - \alpha_4) + \chi_{AB} (2\alpha_8 - \alpha_5) + \frac{1}{n_f} \frac{\chi_A (\chi_S - \chi_A) \ln \chi_A - \chi_B (\chi_S - \chi_B) \ln \chi_B}{\chi_B - \chi_A} \right], \quad (17)$$

where the first term on the RHS is the LO term, the NLO terms being the remaining terms and α_i are the low energy chiral constants (LECs) evaluated at the scale $\Lambda_\chi = 4\pi f_\pi$. With our conventions for the pion decay constant in the chiral limit, f_0 , we have $f_\pi = 92.4 \text{ MeV}$ so that $\Lambda_\chi \approx 1160 \text{ MeV}$.

χ_{AB} are related to the quark masses by [26],

$$\chi_{AB} = \frac{B_0^S (m_A + m_B)^S}{(4\pi f_0)^2}, \quad A, B \in \{V_1, V_2, S\}, \quad (18)$$

where m_S is the sea quark mass and m_{V_i} , $i = 1, 2$ are the (possibly) non-degenerate valence quark masses. In particular we have

$$\chi_{AB} = \frac{1}{2}(\chi_A + \chi_B), \quad \text{where} \quad \chi_A \equiv \chi_{AA}. \quad (19)$$

Furthermore in eq. (18), B_0^S is related to the chiral condensate by

$$B_0^S = -\frac{1}{f_0^2} \langle \bar{q}q \rangle^S. \quad (20)$$

Apart from f_π , none of the other LECs (here B_0 , or $\langle \bar{q}q \rangle$, and $\alpha_4, \alpha_5, \alpha_6, \alpha_8$ in eq. (17)) are well determined. Typical values are (for $n_f = 3$), $\alpha_4 = -0.76(60)$, $\alpha_5 = 0.5(6)$, $\alpha_6 = -0.5(4)$, $\alpha_8 = 0.76(40)$ (as compiled in [27]) giving

$$2\alpha_6 - \alpha_4 \approx -0.24, \quad 2\alpha_8 - \alpha_5 \approx -1.02, \quad \langle \bar{q}q \rangle^{\overline{MS}}(2 \text{ GeV}) \approx -(267 \text{ MeV})^3, \quad (21)$$

(the $\langle \bar{q}q \rangle$ result is taken from [28]).

m_{ps}^{AB} in eq. (17) is the pseudoscalar mass (with $A, B \in \{V_1, V_2\}$) implicitly depending on the sea quark mass m_S . Again for degenerate valence quarks, we write $m_{ps}^A \equiv m_{ps}^{AA}$. Note that we also numerically allow for a valence quark mass to be equal to the sea quark mass, so for example we can write m_{ps}^S .

We shall assume eq. (17) as the basic functional form for the relation between the quark mass and the pseudoscalar mass in the following. As expected this

²The NNLO result has recently been constructed in [24].

equation is symmetric under an interchange of the two valence quarks. However it does not have the most general structure allowed by this symmetry.

Eq. (17) is not very convenient for comparing with numerical results for a variety of reasons (see section 6.1 and eqs. (57), (58)). First, the quantities we measure are not χ_{AB} , m_{ps}^{AB} but only proportional to them,

$$\chi_{AB} = c_\chi y_{AB}, \quad \frac{m_{ps}^{AB}}{4\pi f_0} = c_m M_{ps}^{AB}, \quad (22)$$

where y_{AB} and M_{ps}^{AB} are new variables. Substituting these into eq. (17) simply shifts the coefficients of the various terms (including the 1 and $1/n_f$ terms), while the structural form of this equation remains the same. Note that this includes the cases where c_χ and c_m are functions of the quark mass, e.g.

$$\begin{aligned} c_\chi &\rightarrow c_\chi^{(0)} + c_\chi^{S(1)} y_S + c_\chi^{AB(1)} y_{AB} + \dots, \\ c_m &\rightarrow c_m^{(0)} + c_m^{S(1)} y_S + c_m^{AB(1)} y_{AB} + \dots \end{aligned} \quad (23)$$

Secondly, we prefer to work with a function of the pseudoscalar mass rather than the quark mass, so we invert eq. (17). This gives a functional form, which we choose to write as

$$\begin{aligned} \frac{y_{AB}}{(M_{ps}^{AB})^2} &= c_a + \left(\frac{c_b - c_d(1 + \ln c_a)}{c_a} \right) y_S + \left(\frac{c_c + c_d(1 + 2 \ln c_a)}{c_a} \right) y_{AB} \\ &\quad - \left(\frac{c_d}{c_a} \right) \frac{y_A(y_S - y_A) \ln y_A - y_B(y_S - y_B) \ln y_B}{y_B - y_A}. \end{aligned} \quad (24)$$

Setting $A = B = V$ this equation reduces to the degenerate valence case (and finally setting $V \equiv S$ gives the sea quark case). These sets of equations may be (once) iterated to produce $y_{AB}/(M_{ps}^{AB})^2$ as a function of $(M_{ps}^{AB})^2$ and $(M_{ps}^S)^2$. Relevant later will be the case of degenerate valence quarks when we have

$$\frac{y_V}{(M_{ps}^V)^2} = c_a + c_b (M_{ps}^S)^2 + c_c (M_{ps}^V)^2 + c_d \left((M_{ps}^S)^2 - 2(M_{ps}^V)^2 \right) \ln (M_{ps}^V)^2, \quad (25)$$

which explains our original choice of the c_a, c_i ($i = b, c, d$) coefficients in eq. (24). So, as mentioned previously, we see that determining these coefficients from eq. (25) which only needs degenerate valence quark masses is sufficient to find the results for non-degenerate quark masses, eq. (24).

Numerically we shall find that higher order terms in χ PT are small, i.e. $c_a \gg |c_i| M_{ps}^2$ ($i = b, c, d$) and thus all these manipulations are justified.

The relation between c_χ , c_m and c_a is, from the LO term

$$\frac{c_m^2}{c_\chi} = c_a. \quad (26)$$

At NLO we have in addition

$$c_m^2 = n_f \frac{c_d}{c_a}, \quad (27)$$

and for the remaining LECs the relationships

$$\begin{aligned} 2\alpha_6 - \alpha_4 &= \frac{1}{n_f^2} \left[1 + \ln n_f - \frac{c_b}{c_d} + \ln \frac{c_d}{c_a} \right], \\ 2\alpha_8 - \alpha_5 &= -\frac{1}{n_f} \left[1 + 2 \ln n_f + \frac{c_c}{c_d} + 2 \ln \frac{c_d}{c_a} \right]. \end{aligned} \quad (28)$$

We write the results only for the case when $c_m^{(1)} = c_\chi^{(1)} = 0$ (see eq. (23)). This is sufficient for the later estimation of the LECs in section 6, as we shall be using continuum results³.

Finally we have to find a formula for the strange quark mass. We first note that we have

- Two degenerate sea quarks $m_S \equiv m_{ud} = \frac{1}{2}(m_u + m_d)$
- Three possible valence quarks, m_u , m_d and m_s (where ‘s’ denotes the strange quark). We write $m_u = m_{ud} - \Delta m_{ud}$ and $m_d = m_{ud} + \Delta m_{ud}$ where $\Delta m_{ud} = (m_d - m_u)/2$ is proportional to the difference between the down and up quark masses.

Inputting meson data we use the K^+ ($u\bar{s}$), where we set $A = u$, $B = s$ in eq. (24), K^0 ($d\bar{s}$), where we have $A = d$, $B = s$, and together with the π^+ ($u\bar{d}$), with $A = u$, $B = d$, gives after some algebra the result

$$\begin{aligned} y_s &= c_a \left[M_{K^+}^2 + M_{K^0}^2 - M_{\pi^+}^2 \right] \\ &\quad + (c_b - c_d) \left[M_{K^+}^2 + M_{K^0}^2 \right] M_{\pi^+}^2 \\ &\quad + \frac{1}{2}(c_c + c_d) \left[M_{K^+}^2 + M_{K^0}^2 \right]^2 \\ &\quad - (c_b + c_c) M_{\pi^+}^4 \\ &\quad - c_d \left[M_{K^+}^2 + M_{K^0}^2 \right] \left[M_{K^+}^2 + M_{K^0}^2 - M_{\pi^+}^2 \right] \ln \left(M_{K^+}^2 + M_{K^0}^2 - M_{\pi^+}^2 \right) \\ &\quad + c_d M_{\pi^+}^4 \ln M_{\pi^+}^2 + \dots, \end{aligned} \quad (29)$$

for the strange quark and

$$y_{ud} = c_a M_{\pi^+}^2 + (c_b + c_c) M_{\pi^+}^4 - c_d M_{\pi^+}^4 \ln M_{\pi^+}^2 + \dots, \quad (30)$$

³For the more general case in eqs. (26), (27) and (28) c_m , c_χ are replaced by $c_m^{(0)}$ and $c_\chi^{(0)}$ respectively, together with additional terms on the RHS of eq. (28) of $-1/(n_f(c_\chi^{(0)})^2)(c_\chi^{S(1)} - 2c_m^{S(1)}/c_m^{(0)})$ and $-1/(c_\chi^{(0)})^2(c_\chi^{AB(1)} - 2c_m^{AB(1)}/c_m^{(0)})$ for the second and third equations, respectively.

for the light quark, where the \dots include higher order terms in χ PT (i.e. NNLO) and terms of $O((\Delta m_{ud})^2)$.

The results of eqs. (29) and (30) are valid for ‘pure’ QCD. To include electromagnetic effects, we use Dashen’s theorem which says that if electromagnetic effects are the only source of breaking of isospin symmetry (i.e. $m_u = m_d$), the leading electromagnetic contribution to $m_{K^+}^2$ and $m_{\pi^+}^2$ are equal while $m_{\pi^0}^2$ and $m_{K^0}^2$ are unaffected (see e.g. [29]). Thus the masses in eqs. (29) and (30) may be written as [30]

$$\begin{aligned} m_{K^+}^2 &= (m_{K^+}^{EXPT})^2 - (m_{\pi^+}^{EXPT})^2 + (m_{\pi^0}^{EXPT})^2, \\ m_{K^0}^2 &= (m_{K^0}^{EXPT})^2, \\ m_{\pi^+}^2 = m_{\pi^0}^2 &= (m_{\pi^0}^{EXPT})^2. \end{aligned} \tag{31}$$

where m_{K^+} , m_{K^0} , m_{π^+} and m_{π^0} are the ‘pure’ QCD numbers, while $m_{K^+}^{EXPT}$, $m_{K^0}^{EXPT}$, $m_{\pi^+}^{EXPT}$ and $m_{\pi^0}^{EXPT}$ are the experimentally observed numbers. Dashen’s theorem has corrections $O(\alpha_{QED} m_q)$ from higher order terms in χ PT, estimates vary as to the magnitude of this correction [31, 32], see [30, 33] for a discussion. Recent results from the lattice approach [34, 35] seem to indicate only a mild breaking of Dashen’s theorem.

Note that to LO in χ PT using experimental values of the π and K masses, namely

$$\begin{aligned} m_{\pi^+}^{EXPT} &= 139.6 \text{ MeV} & m_{\pi^0}^{EXPT} &= 135.0 \text{ MeV}, \\ m_{K^+}^{EXPT} &= 493.7 \text{ MeV} & m_{K^0}^{EXPT} &= 497.7 \text{ MeV}, \end{aligned} \tag{32}$$

we have the result

$$\begin{aligned} \frac{m_s^S(M)}{m_{ud}^S(M)} &= \frac{m_{K^+}^2 + m_{K^0}^2 - m_{\pi^+}^2}{m_{\pi^+}^2} \\ &= \frac{(m_{K^+}^{EXPT})^2 + (m_{K^0}^{EXPT})^2 - (m_{\pi^+}^{EXPT})^2}{(m_{\pi^0}^{EXPT})^2} \approx 25.9, \end{aligned} \tag{33}$$

independent of the value of c_a . So if we are in or close to this regime, once we have determined the strange quark mass, this immediately gives an estimate of the light quark mass. Incorporating the NLO terms needs a determination of all the c_a and c_i ($i = b, c, d$) coefficients in eqs. (29), (30) and gives the results in section 6.2.

4 The Lattice Approach

Here we shall derive results for the unquenched ($n_f = 2$) strange quark mass using the axial Ward identity. All our numerical computations are done with degenerate valence quark masses.

The starting point is the AWI; in the continuum we have the renormalised relation

$$\partial_\mu \mathcal{A}_\mu^{\mathcal{R}} = 2m_q^{\mathcal{S}}(M)\mathcal{P}^{\mathcal{S}}(M), \quad (34)$$

where $\mathcal{A}^{\mathcal{R}}$ and $\mathcal{P}^{\mathcal{S}}$ are the renormalised (in scheme \mathcal{S}) axial current and pseudoscalar density respectively. In the (bare) lattice theory the current quark masses are also defined via the equivalent AWI⁴

$$\partial_\mu^{LAT} \mathcal{A}_\mu = 2\widetilde{m}_q \mathcal{P} + O(a^2), \quad (35)$$

where \mathcal{A} and \mathcal{P} are the $O(a)$ improved unrenormalised axial current and pseudoscalar density

$$\begin{aligned} \mathcal{A}_\mu &= (1 + b_A am_q)(A_\mu + c_A a \partial_\mu^{LAT} P), \\ \mathcal{P} &= (1 + b_P am_q)P, \end{aligned} \quad (36)$$

with

$$A_\mu = \bar{q}\gamma_\mu\gamma_5 q, \quad P = \bar{q}\gamma_5 q. \quad (37)$$

Wilson-type fermions allow several different definitions of the quark mass. We denote the (bare) quark mass defined from the AWI with a tilde, $a\widetilde{m}_q$, while that from the VWI is given by

$$am_q = \frac{1}{2} \left(\frac{1}{\kappa_q} - \frac{1}{\kappa_{qc}^{\mathcal{S}}} \right), \quad (38)$$

where κ_q is the Wilson hopping parameter, defining the quark mass (both sea and valence). The critical sea quark hopping parameter, $\kappa_{qc}^{\mathcal{S}}$, is defined for fixed $\beta \equiv 6/g_0^2$ (where g_0 is the lattice coupling) by the vanishing of the pseudoscalar mass⁵, i.e. $m_{ps}|_{\kappa_q=\kappa_{qc}^{\mathcal{S}}} = 0$.

Returning to eq. (36), c_A is known non-perturbatively [36], but not b_A and b_P . However results using one-loop perturbation theory [37], or for non-perturbative quenched QCD [38], show that the difference $b_A - b_P$ is small (there is however an increase between the perturbative and quenched non-perturbative results). Multiplying by am_q thus gives a correction of perhaps half a percent, which with our present level of accuracy we can ignore.

Forming lattice correlation functions means that the quark mass can be defined and determined from the ratio⁶

$$a\widetilde{m}_q \stackrel{t \gg 0}{\cong} \frac{\langle \partial_4^{LAT} \mathcal{A}_4(t) \mathcal{O}(0) \rangle}{2\langle \mathcal{P}(t) \mathcal{O}(0) \rangle}$$

⁴ ∂_μ^{LAT} is the symmetric lattice derivative, conventionally chosen to be $(\partial_\mu^{LAT} f)(x) = [f(x + a\hat{\mu}) - f(x - a\hat{\mu})]/(2a)$, where $\hat{\mu}$ is a unit vector in the μ direction.

⁵We shall suppress the ‘V’ superscript on the pseudoscalar mass and only include an ‘S’ superscript where necessary.

⁶Note that to reduce noise, derivatives of operators on the lattice are taken as compact as possible, consistent with the given symmetry. Thus we use, no μ summation, $(\partial_\mu^2 f)(x) = [f(x + a\hat{\mu}) - 2f(x) + f(x - a\hat{\mu})]/(2a)^2 = (\partial_\mu^{LAT} \partial_\mu^{LAT} f)(x) + O(a)$.

β	κ_q^S	c_{sw}	V	Group
5.20	0.1342	2.0171	$16^3 \times 32$	QCDSF
5.20	0.1350	2.0171	$16^3 \times 32$	UKQCD
5.20	0.1355	2.0171	$16^3 \times 32$	UKQCD
5.25	0.1346	1.9603	$16^3 \times 32$	QCDSF
5.25	0.1352	1.9603	$16^3 \times 32$	UKQCD
5.25	0.13575	1.9603	$24^3 \times 48$	QCDSF
5.29	0.1340	1.9192	$16^3 \times 32$	UKQCD
5.29	0.1350	1.9192	$16^3 \times 32$	QCDSF
5.29	0.1355	1.9192	$24^3 \times 48$	QCDSF
5.29	0.1359	1.9192	$24^3 \times 48$	QCDSF
5.40	0.1350	1.8228	$24^3 \times 48$	QCDSF
5.40	0.1356	1.8228	$24^3 \times 48$	QCDSF
5.40	0.1361	1.8228	$24^3 \times 48$	QCDSF

Table 2: The β , κ_q^S and c_{sw} values⁸ and the lattice volume $V \equiv N_S^3 \times N_T$. The collaboration that generated the configurations is given in the last column.

$$\begin{aligned}
&\approx \frac{\langle \partial_4^{LAT} A_4(t) \mathcal{O}(0) \rangle}{2 \langle \mathcal{P}(t) \mathcal{O}(0) \rangle} + c_A a \frac{\langle \partial_4^{2LAT} P(t) \mathcal{O}(0) \rangle}{2 \langle \mathcal{P}(t) \mathcal{O}(0) \rangle} + O(a^2) \\
&\equiv a \widetilde{m}_q^{(0)} + c_A a \widetilde{m}_q^{(1)} + O(a^2), \tag{39}
\end{aligned}$$

where \approx in the second equation signifies that we have dropped the correction factor $1 + (b_A - b_P)am_q$. \mathcal{O} is an operator with a non-zero overlap with the pseudoscalar particle. We choose it here to be P^{smear} , where we have used Jacobi smearing (see the appendix) on the operator.

The parameter space spanned in our numerical simulations is given in Table 2. The notation is standard for the parameters of the action, see for example [40]. (The critical Wilson hopping parameters, κ_{qc}^S , have been determined in [11] for each β .)

In the appendix we list our κ_q for each κ_q^S together with the corresponding partially quenched am_{ps} and bare AWI quark masses $a\widetilde{m}_q^{(0)}$, $a\widetilde{m}_q^{(1)}$ and $a\widetilde{m}_q$.

5 Renormalisation

5.1 Generalities

Imposing the AWI on the lattice, eq. (35), up to cut-off effects means that the axial current as well as the pseudoscalar density and the quark mass must be

⁸For the number of trajectories generated for each κ_q^S , see for example [39].

renormalised. Thus we have

$$\mathcal{A}_\mu^{\mathcal{R}} = Z_A \mathcal{A}_\mu, \quad \mathcal{P}^{\mathcal{S}}(M) = Z_P^{\mathcal{S}}(M) \mathcal{P}, \quad (40)$$

giving

$$m_q^{\mathcal{S}}(M) = Z_{\tilde{m}}^{\mathcal{S}}(M) \tilde{m}_q, \quad Z_{\tilde{m}}^{\mathcal{S}}(M) = \frac{Z_A}{Z_P^{\mathcal{S}}(M)}, \quad (41)$$

or in RGI form

$$m_q^{\text{RGI}} = Z_{\tilde{m}}^{\text{RGI}} \tilde{m}_q, \quad Z_{\tilde{m}}^{\text{RGI}} = \Delta Z_m^{\mathcal{S}}(M) Z_{\tilde{m}}^{\mathcal{S}}(M). \quad (42)$$

5.2 Non Perturbative renormalisation

We shall employ here the RI'-MOM scheme [41], which is easily transcribed to the lattice. Our implementation of this method is described in [42]. As discussed in section 2 to obtain the RGI quark mass, we must determine both $\Delta Z_m^{\text{RI}'-MOM}$ and $Z_{\tilde{m}}^{\text{RI}'-MOM}$. The RGI quark mass can then be easily converted back to the $\overline{\text{MS}}$ scheme.

5.2.1 $\Delta Z_m^{\text{RI}'-MOM}$

We start with $\Delta Z_m^{\text{RI}'-MOM}$. To write down the perturbative expansion, a definition of the coupling constant is required. The anomalous dimension coefficients have been determined to fourth order in [41, 43, 44] by taking the coupling constant to be $g^{\overline{\text{MS}}}$. Thus the anomalous dimension function is considered as a function of $g^{\overline{\text{MS}}}$. (Other definitions of the coupling constant are possible, more closely related to MOM schemes [45].) So we write

$$\gamma_m^{\text{RI}'-MOM}(g^{\overline{\text{MS}}}) = d_{m0}(g^{\overline{\text{MS}}})^2 + d_{m1}^{\text{RI}'-MOM}(g^{\overline{\text{MS}}})^4 \dots, \quad (43)$$

with coefficients given by [44],

$$\begin{aligned} d_{m1}^{\text{RI}'-MOM} &= -\frac{2}{(4\pi)^4} \left[126 - \frac{52}{9} n_f \right], \\ d_{m2}^{\text{RI}'-MOM} &= -\frac{2}{(4\pi)^6} \left[\frac{20174}{3} - \frac{3344}{3} \zeta_3 - \left(\frac{17588}{27} - \frac{128}{9} \zeta_3 \right) n_f + \frac{856}{81} n_f^2 \right], \\ d_{m3}^{\text{RI}'-MOM} &= -\frac{2}{(4\pi)^8} \left[\frac{141825253}{324} - \frac{7230017}{54} \zeta_3 + \frac{6160}{3} \zeta_5 \right. \\ &\quad \left. - \left(\frac{3519059}{54} - \frac{298241}{27} \zeta_3 - \frac{4160}{3} \zeta_5 \right) n_f \right. \\ &\quad \left. + \left(\frac{611152}{243} - \frac{5984}{27} \zeta_3 \right) n_f^2 - \frac{16024}{729} n_f^3 \right], \end{aligned} \quad (44)$$

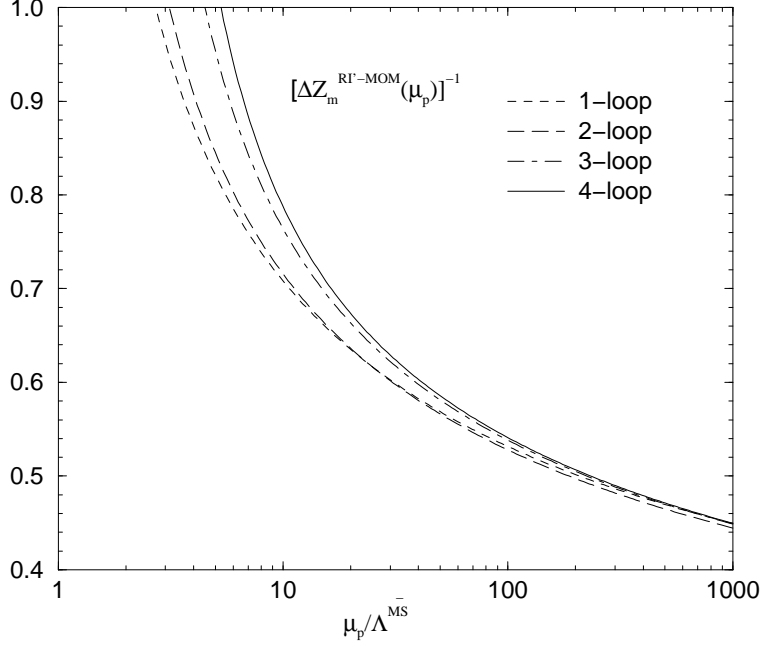


Figure 2: $[\Delta Z_m^{RI'-MOM}(\mu_p)]^{-1}$ versus $\mu_p/\Lambda^{\overline{MS}}$.

which allows $[\Delta Z_m^{RI'-MOM}(\mu_p)]^{-1}$, where μ_p is taken to be the momentum scale in this scheme, to be computed in the usual way,

$$[\Delta Z_m^{RI'-MOM}(\mu_p)]^{-1} = [2b_0 g^{\overline{MS}}(\mu_p)^2]^{-\frac{d_{m0}}{2b_0}} \exp \left\{ \int_0^{g^{\overline{MS}}(\mu_p)} d\xi \left[\frac{\gamma_m^{RI'-MOM}(\xi)}{\beta^{\overline{MS}}(\xi)} + \frac{d_{m0}}{b_0 \xi} \right] \right\}. \quad (45)$$

(This result may also be shown by changing the integration variable in eq. (9) from some defined $g^{RI'-MOM}$ to $g^{\overline{MS}}$, by using eq. (10), i.e. $g^{RI'-MOM}(\mu_p) = G(g^{\overline{MS}}(\mu_p))$.)

In Fig. 2 we show $[\Delta Z_m^{RI'-MOM}]^{-1}$ as a function of $\mu_p/\Lambda^{\overline{MS}}$. The convergence for $\Delta Z_m^{RI'-MOM}$ seems slightly worse in the region of interest than that for the corresponding $\Delta Z_m^{\overline{MS}}$ as there is more of a change from the 2-loop to 3-loop result (see Fig. 1 for a comparison with $\Delta Z_m^{\overline{MS}}$). However this is mitigated by the extraction of RI'-MOM being performed at a range of scales including higher scales than 2 GeV. Thus, for example, a typical value of $(a\mu_p)^2 \approx 4$ (see Fig. 4) corresponds to $\mu_p/\Lambda^{\overline{MS}} \gtrsim 20$ where the convergence (between the 3-loop and 4-loop results) appears to be better.

5.2.2 $Z_{\tilde{m}}^{RI'-MOM}$

The RI'-MOM scheme considers amputated Green's functions (practically in the Landau gauge) with an appropriate operator insertion, here either A or P . The renormalisation point is fixed at some momentum scale $p^2 = \mu_p^2$, and thus we

have, e.g. [41, 42],

$$Z_O^{RI'-MOM}(\mu_p) = \frac{Z_q^{RI'-MOM}(p)}{\frac{1}{12} \text{tr} [\Gamma_O(p) \Gamma_{O,BORN}^{-1}(p)]} \Bigg|_{p^2=\mu_p^2} \quad (46)$$

where Γ_O are one-particle irreducible (1PI) vertex functions, and Z_q is the wave-function renormalisation. We have generated Γ_O only at values of the sea quark mass, i.e. the values in Table 2.

To obtain $Z_{\tilde{m}}^{RI'-MOM}$ we need both Z_A and $Z_P^{RI'-MOM}$ in the chiral limit. Z_A is unproblematical, we make a linear fit of the form

$$Z_A = A_A + B_A am_q, \quad (47)$$

where am_q is defined in eq. (38) and κ_{qc}^S has been determined in [11].

From the Ward identity obeyed by Γ_P , we expect, due to chiral symmetry breaking, that $Z_P^{RI'-MOM}$ develops a pole in the quark mass. Hence we have $Z_P \rightarrow 0$ with the quark mass. Thus following [46] we try a fit of the form⁹

$$(Z_P^{RI'-MOM})^{-1} = A_P + \frac{B_P}{am_q}. \quad (48)$$

From the operator product expansion [47, 48] we expect

$$B_P(\mu_p) \propto \frac{1}{(a\mu_p)^2}, \quad (49)$$

where the constant of proportionality is proportional to the chiral condensate. Thus we see that as the scale increases, the B_P coefficient decreases.

A chiral extrapolation using eqs. (47) and (48) has been made using only the sea data sets to determine the functions $A_A(\mu_p)$ and $A_P(\mu_p)$ respectively. The lattice momenta originally chosen for the heaviest quark masses were kept fixed for the extrapolation over the different masses. If another data set did not have a particular momentum a linear interpolation was performed between the adjacent momenta straddling the given momentum.

Results for $Z_P^{RI'-MOM}$ are shown for $\beta = 5.20, 5.40$ in Fig. 3. B_P is small and decreasing with increasing $(a\mu_p)^2$ as required from eq. (49). (Note that numerically, there is evidence for a term of the form B_P/am_q as attempting a linear extrapolation, as for Z_A in eq. (47), gave a substantial increase in the fit χ^2 .) Although we do not determine the chiral condensate [49] in this section (see section 6.1), we note that numerically the Goldstone pion contamination to Γ_P appears to be small [50].

⁹It made little difference to the A_P (or A_A) coefficients whether $a\tilde{m}_q$ or $(am_{ps})^2$ is used.

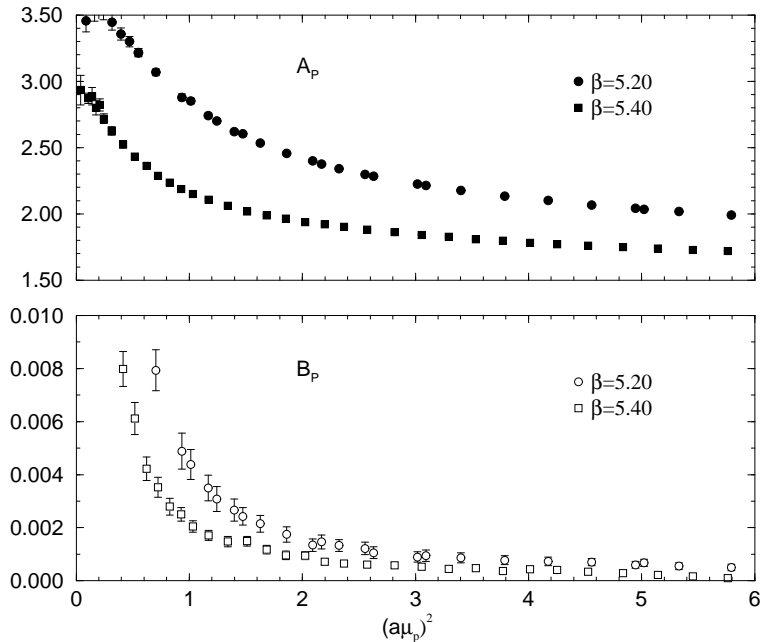


Figure 3: A_P and B_P for $Z_P^{RI'-MOM}$ for $\beta = 5.20$, and $\beta = 5.40$.

β	$Z_{\tilde{m}}^{RCI}$
5.20	2.270(12)
5.25	2.191(24)
5.29	2.177(14)
5.40	2.124(06)

Table 3: Values of $Z_{\tilde{m}}^{RCI}$ from the NP method of section 5.2.3.

5.2.3 $Z_{\tilde{m}}^{RCI}$

Taking these values for $A_A \equiv Z_A$ and $A_P \equiv Z_P^{RI'-MOM}$, forming the ratio $Z_A/Z_P^{RI'-MOM}$ and multiplying by $\Delta Z_m^{RI'-MOM}$ will then give $Z_{\tilde{m}}^{RCI}$. This should be independent of $(a\mu_p)^2$. Some results are shown in Fig. 4. Due to cut-off effects, non-perturbative contributions etc., they are not quite constant although the curves become flatter for increasing β . To allow for the non-constant remnants we make a phenomenological fit of the form

$$F(a\mu_p) = r_1 + r_2(a\mu_p)^2 + \frac{r_3}{(a\mu_p)^2}, \quad (50)$$

where we associate $Z_{\tilde{m}}^{RCI}$ with r_1 . This gives the results in Table 3. We start the fit range at $(a\mu_p)^2 = 1.5$, the fit results for r_1 were found to be insensitive to decreasing the fit range.

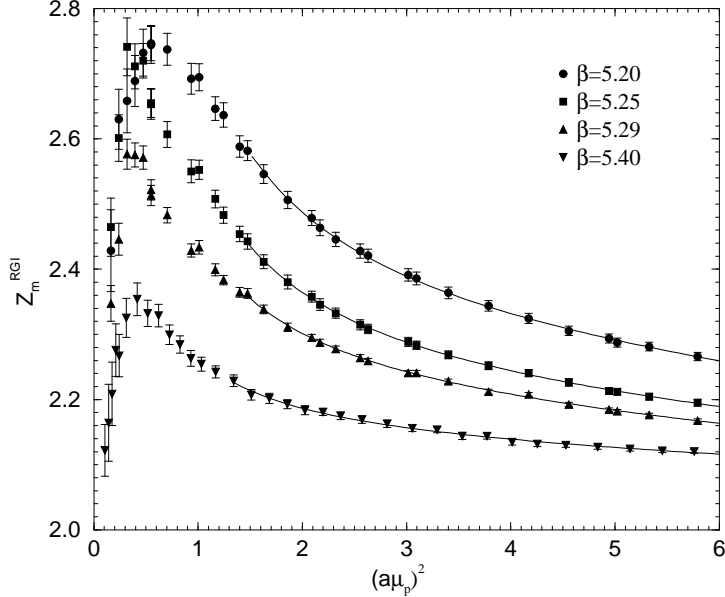


Figure 4: $Z_{\tilde{m}}^{\text{RGI}}$ for $\beta = 5.20$ (filled circles), $\beta = 5.25$ (filled squares), $\beta = 5.29$ (filled upper triangles), $\beta = 5.40$ (filled lower triangles) together with fits as in eq. (50).

5.3 Comparison of $Z_{\tilde{m}}^{\text{RGI}}$ with other results

As many computations of the strange quark mass have used tadpole improved perturbation theory together with a boosted coupling constant for the determination of the renormalisation constant, it is of interest to compare our results obtained in the previous section with this approach. Our variation of this method, tadpole-improved renormalisation-group-improved boosted perturbation theory or TRB-PT, is described in [51, 40]. Here we recapitulate the method. Regarding the lattice as a ‘scheme’, then from eq. (8) we can write

$$m_q^{\text{RGI}} = \Delta Z_{\tilde{m}}^{\text{LAT}}(a) \tilde{m}_q(a), \quad (51)$$

where the renormalisation-group-improved $\Delta Z_{\tilde{m}}^{\text{LAT}}(a)$ is given by eq. (9). Furthermore in this ‘lattice’ scheme, we choose to use $g_{\square}^2 = g_0^2/u_{0c}^4$ where $u_0^4 = \langle \frac{1}{3} \text{Tr} U^{\square} \rangle$ (U^{\square} being the product of links around an elementary plaquette) rather than g_0 , as series expansions in g_{\square} are believed to have better convergence. This is boosted perturbation theory. (We shall use chirally extrapolated plaquette values as determined in [19] at our β values and so we add a subscript ‘c’ to u_0 .) In the tadpole-improved, or mean field approximation, renormalisation constants for operators with no derivatives are $\propto u_{0c}$, which indicates that $Z_{\tilde{m}}^{\text{RGI}} u_{0c}^{-1}$ will

β	$Z_{\tilde{m}}^{RGI(TRB-PT)}$
5.20	1.837
5.25	1.851
5.29	1.862
5.40	1.891

Table 4: Values of $Z_{\tilde{m}}^{RGI(TRB-PT)}$ from section 5.3.

converge faster than $Z_{\tilde{m}}^{RGI}$ alone so we re-write the two-loop equation eq. (11) as¹⁰

$$Z_{\tilde{m}}^{RGI(TRB-PT)} \equiv \Delta Z_{\tilde{m}}^{LAT}(a) = u_{0c} \left[2b_0 g_{\square}^2 \right]^{\frac{d_{m0}}{2b_0}} \left[1 + \frac{b_1}{b_0} g_{\square}^2 \right]^{\frac{b_0 d_{\tilde{m}1}^{LAT} - b_1 d_{m0}}{2b_0 b_1} + \frac{p_1}{4} \frac{b_0}{b_1}}, \quad (52)$$

where p_1 is the first coefficient in the expansion of u_{0c} , i.e. $u_{0c} = 1 - \frac{1}{4}g_0^2 p_1 + \dots$ with $p_1 = \frac{1}{3}$.

It remains to determine $d_{\tilde{m}1}^{LAT}$. This may be found by relating the (known) perturbative result for $Z_{\tilde{m}}^{\overline{MS}}$ to $\Delta Z_{\tilde{m}}^{LAT}$ (for simplicity at the scale $\mu = 1/a$) by

$$Z_{\tilde{m}}^{\overline{MS}}(1/a) = \frac{\Delta Z_{\tilde{m}}^{LAT}(a)}{\Delta Z_{\tilde{m}}^{\overline{MS}}(1/a)} = 1 - g_0^2 B_{\tilde{m}}^{\overline{MS}}(1) + \dots, \quad (53)$$

where

$$B_{\tilde{m}}^{\overline{MS}}(c_{sw}) = \frac{4/3}{(4\pi)^2} \left(-6.79916 + 2.4967c_{sw} - 4.28739c_{sw}^2 \right). \quad (54)$$

This result for $B_{\tilde{m}}^{\overline{MS}} \equiv B_A - B_P^{\overline{MS}}$ is taken from [52]. (Indeed we could alternatively consider TRB-PT for Z_A and $Z_P^{\overline{MS}}$ separately and then form the ratio. The results turned out to be about 1% lower than those presented here.)

Expanding the ratio in eq. (53), by using the results in eqs. (52) and (11) for the ‘lattice’ and \overline{MS} schemes respectively and t_1 , defined in eq. (10) (which using the notation of [19] is numerically given by $t_1 = t_1^{LAT}(1)$, with $t_1^{LAT}(c_{sw}) = 0.4682013 - n_f(0.0066960 - 0.0050467c_{sw} + 0.0298435c_{sw}^2)$) gives finally

$$d_{\tilde{m}1}^{TRB-PT} = d_{\tilde{m}1}^{\overline{MS}} + d_{m0}(t_1 - p_1) - 2b_0 B_{\tilde{m}}^{\overline{MS}}(1) \equiv -\frac{4.04873}{(4\pi)^4}. \quad (55)$$

Thus from eq. (52) various values of $\Delta Z_{\tilde{m}}^{LAT}$, or equivalently $Z_{\tilde{m}}^{RGI(TRB-PT)}$, can be found. Results are given in Table 4.

We now turn to a comparison of the results. In Fig. 5 we plot $Z_{\tilde{m}}^{RGI}$ versus β . Our NP results from section 5.2 are shown as filled circles. They are to

¹⁰The TRB-PT subscript in brackets is there only to distinguish the results from those obtained in section 5.2.

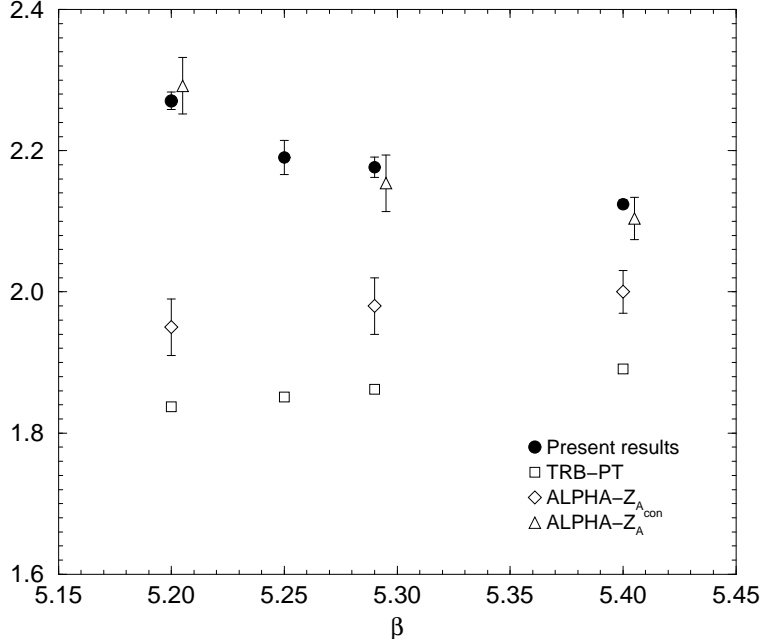


Figure 5: $Z_{\tilde{m}}^{RGI}$ versus β . The black circles are the results from Table 3, while the open squares are the TRB-PT results from Table 4. Furthermore the open diamonds and triangles are the NP results from [12], using the two different results for the axial renormalisation constant, [53]. (The empty triangle results has been slightly displaced for clarity.)

be compared with the TRB-PT results denoted by empty squares. While there is a difference between the results, it is decreasing for $\beta \rightarrow \infty$ and thus may be primarily due to remnant $O(a^2)$ effects, which disappear in the continuum limit. That various determinations of $Z_{\tilde{m}}^{RGI}$ have different numerical values can be seen from the results of [12] (open diamonds and triangles). In these results two different definitions of the axial renormalisation constant have been used, [53]. Z_A is computed when dropping certain disconnected diagrams, while Z_A^{CON} includes them. The difference between the two definitions is an $O(a^2)$ effect. Using Z_A^{CON} in $Z_{\tilde{m}}^{RGI}$ leads, perhaps coincidentally, to very similar results to our NP results.

Investigating the possibility of $O(a^2)$ differences a little further, we note that if we have two definitions of $Z_{\tilde{m}}^{RGI}$ then if both are equally valid, forming the ratio should yield

$$R_{\tilde{m}}^X \equiv \frac{Z_{\tilde{m}}^{RGI(X)}}{Z_{\tilde{m}}^{RGI}} = 1 + O(a^2), \quad (56)$$

where $Z_{\tilde{m}}^{RGI}$ is the result of section 5.2 and X is some alternative definition (i.e. TRB-PT, ALPHA- Z_A , ALPHA- Z_A^{CON}). In Fig. 6 we plot this ratio for these alternative definitions. The r_0/a values used for the x -axis are found by extrap-

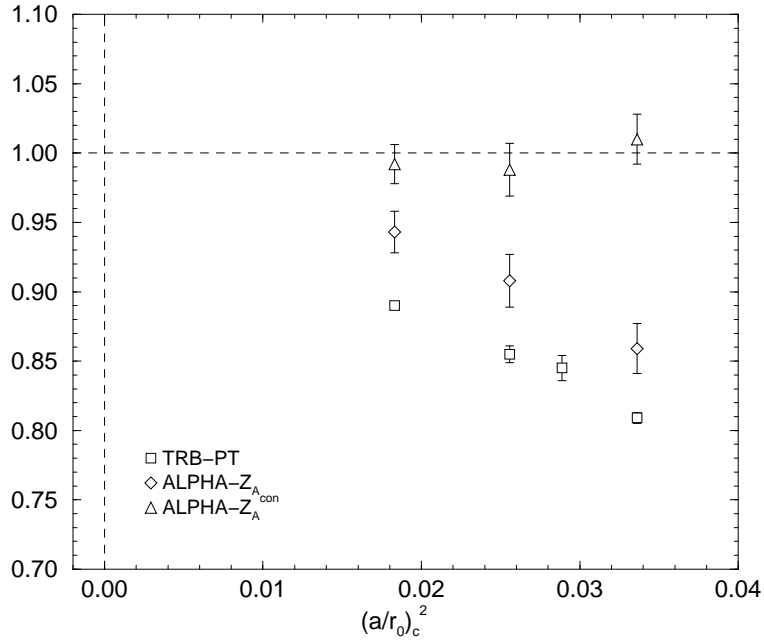


Figure 6: R_m^X versus $(a/r_0)_c^2$ for $X = \text{TRB-PT}$ (open squares), $X = \text{ALPHA-}Z_A$ (open diamonds) and $X = \text{ALPHA-}Z_A^{CON}$ (open triangles).

olating the r_0/a results to the chiral limit. This extrapolation and results for $(r_0/a)_c$ are given in [19].

We see that (roughly) all three ratios extrapolate to 1 which implies that any of the four determinations of $Z_{\tilde{m}}^{RCI}$ may be used. This includes the TRB-PT result. Of course other TI determinations might not have this property, and also their validity always has to be checked against a NP determination, so this result here is of limited use; it is always essential to make a NP determination of the renormalisation constant. Furthermore it is also to be noted that different determinations can have rather different $O(a^2)$ corrections, so a continuum extrapolation is always necessary.

6 Results

6.1 Generalities

In Figs. 7, 8, 9 and 10 we plot the ratio $r_0 m_q^{RCI} / (r_0 m_{ps})^2$ against $(r_0 m_{ps})^2$, where $r_0 \equiv r_0^S$. (i.e. r_0 depends only on the sea quark mass, S). The numerical values of r_0/a are given in [19], Table 2. r_0 seems to be a good scale to use because this ratio numerically does not vary much, as can be seen from the figures.

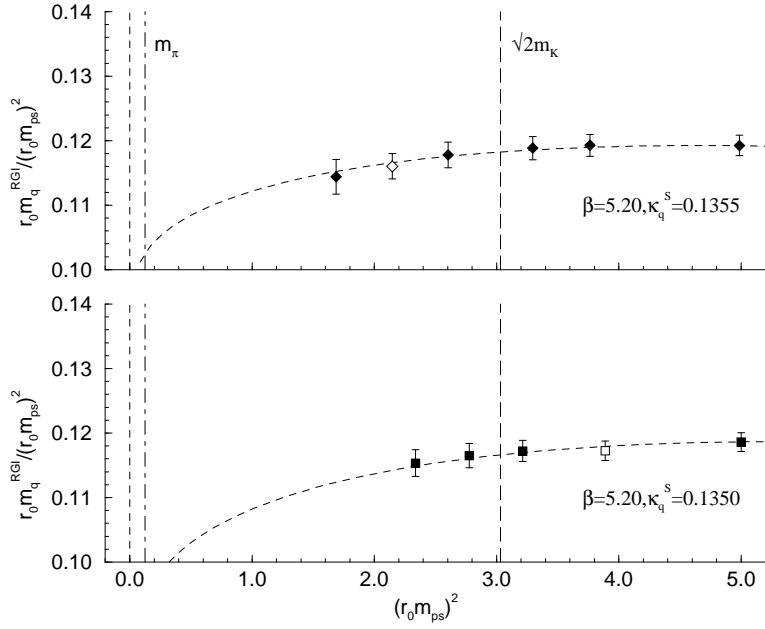


Figure 7: The ratio $r_0 m_q^{RGI} / (r_0 m_{ps})^2$ against $(r_0 m_{ps})^2$ for $\beta = 5.20$. The fit is described in the text. Results for equal sea and valence quark masses are denoted by an open symbol; partially quenched results by filled symbols. The labelled dashed and dashed-dotted lines are also explained in the text.

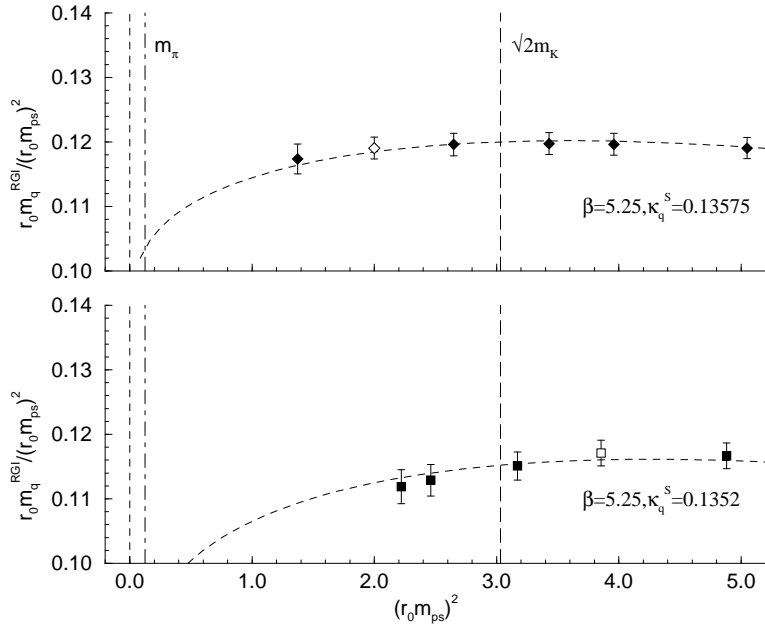


Figure 8: The ratio $r_0 m_q^{RGI} / (r_0 m_{ps})^2$ against $(r_0 m_{ps})^2$ for $\beta = 5.25$. Notation as for Fig. 7.

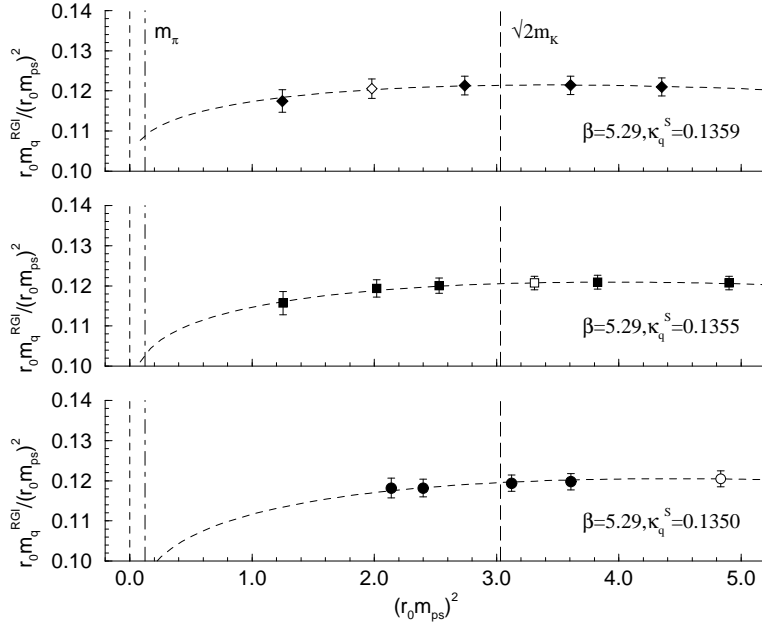


Figure 9: The ratio $r_0 m_q^{RGI} / (r_0 m_{ps})^2$ against $(r_0 m_{ps})^2$ for $\beta = 5.29$. Notation as for Fig. 7.

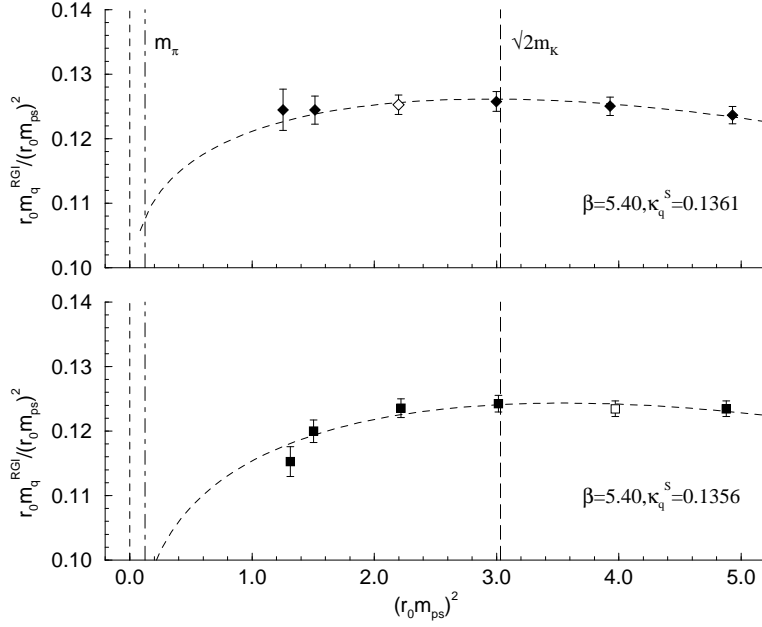


Figure 10: The ratio $r_0 m_q^{RGI} / (r_0 m_{ps})^2$ against $(r_0 m_{ps})^2$ for $\beta = 5.40$. Notation as for Fig. 7.

β	c_a^{RGI}	c_b^{RGI}	c_c^{RGI}	c_d^{RGI}
5.20	0.1115(53)	-0.00227(187)	0.00557(491)	0.00121(133)
5.25	0.1169(42)	-0.00428(160)	0.00612(399)	0.00153(111)
5.29	0.1166(29)	-0.00199(117)	0.00470(287)	0.00121(090)
5.40	0.1218(24)	-0.00324(079)	0.00646(179)	0.00189(056)
∞	0.1330(74)	-0.00378(254)	0.00789(607)	0.00275(179)

Table 5: Values of c_a^{RGI} and c_i^{RGI} ($i = b, c, d$) together with their extrapolated (continuum) values ($\beta = \infty$).

Using eq. (25) (the case of degenerate valence quarks) we set

$$y_V = r_0 m_q^{RGI}, \quad M_{ps}^S = r_0 m_{ps}^S, \quad M_{ps}^V = r_0 m_{ps}, \quad (57)$$

to give a fit equation of the form

$$\frac{r_0 m_q^{RGI}}{(r_0 m_{ps})^2} = c_a^{RGI} + c_b^{RGI} (r_0 m_{ps}^S)^2 + c_c^{RGI} (r_0 m_{ps})^2 + c_d^{RGI} \left((r_0 m_{ps}^S)^2 - 2(r_0 m_{ps})^2 \right) \ln(r_0 m_{ps})^2. \quad (58)$$

We use this equation to determine the coefficients c_a^{RGI} and c_i^{RGI} , $i = b, c, d$. The coefficients depend only on lattice simulation quantities and the unit chosen, and not on the scale as given for example in eq. (15) or eq. (16). This can be useful, as an aid, when making comparisons with other results.

As already mentioned, up to this order in chiral perturbation theory no input from lattice simulations with non-degenerate valence quark masses is needed. To test also numerically that the effects from non-degenerate quark masses are indeed small, we calculated correlation functions using non-degenerate valence quark masses $m_q^A \neq m_q^B$ as well as degenerate valence quark masses with $m_q^S \equiv (m_q^A + m_q^B)/2$. We found the relevant quantities am_{ps} and $a\tilde{m}_q$ to differ by $\lesssim 1\%$.

In Figs. 7, 8, 9 and 10 the dashed lines (labelled ' $\sqrt{2}m_K$ ') represent a fictitious particle composed of two strange quarks, which at LO χ PT gives from eq. (29) (or equivalently eq. (63)) the line $(r_0 m_{ps})^2 \equiv (r_0 m_{K^+})^2 + (r_0 m_{K^0})^2 - (r_0 m_{\pi^+})^2$, while the dashed-dotted lines (labelled ' m_π ') represent a fictitious pion with mass degenerate u and d quarks given from eq. (30) (or equivalently eq. (64)) by $(r_0 m_{\pi^+})^2$.

The presence of a chiral logarithm in the data manifests itself in the bending of the results for smaller quark mass, which can be seen in Figs. 7, 8, 9 and 10. Results for the fit parameters are given in Table 5.

Numerically we expect the leading order in χ PT to be dominant with the NLO giving only minor corrections¹¹, i.e. we expect $c_a^{RGI} \gg (r_0 m_{ps})^2 c_i^{RGI}$ ($i = b, c, d$) and this is indeed found. Using these results for c_a^{RGI} , c_i^{RGI} ($i = b, c, d$) in Fig. 11 we

¹¹Alternative plots, using constant a so $a\tilde{m}_q/(am_{ps})^2$ against $(am_{ps})^2$ or equivalently

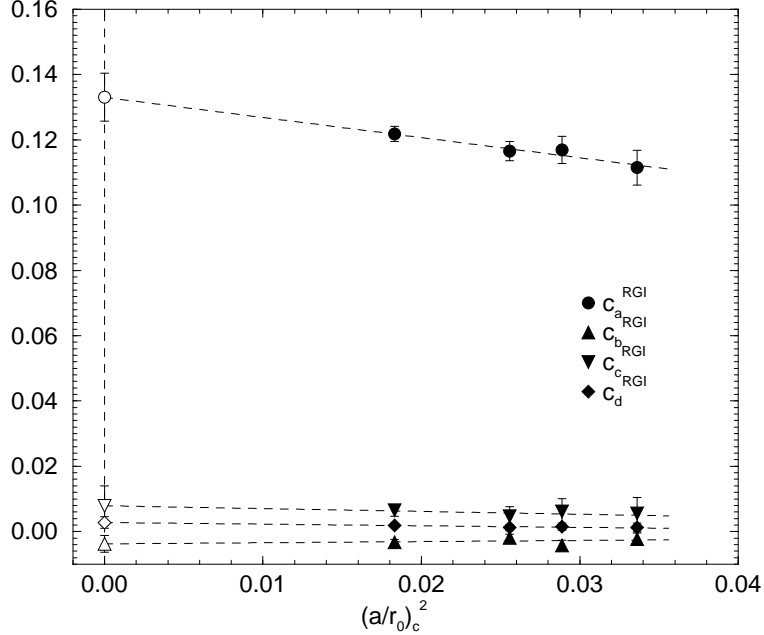


Figure 11: c_a^{RGI} (filled circles), c_b^{RGI} (filled upper triangles) c_c^{RGI} (filled lower triangles) and c_d^{RGI} (filled diamonds) versus $(a/r_0)_c^2$. The $(r_0/a)_c$ i.e. the chirally extrapolated values for r_0/a are used. The open symbols represent the values of c_a^{RGI} and c_i^{RGI} ($i = b, c, d$) in the continuum limit.

present their continuum extrapolations. The r_0/a values used for the x -axis are found by extrapolating the previously used r_0/a results to the chiral limit. This extrapolation and results (for $(r_0/a)_c$) are also given in [19]. This gives values in the last line of Table 5 ($\beta = \infty$).

As a first check on these results and to find some idea of possible systematic effects, we have varied the fit interval from the chosen $(r_0 m_{ps})^2 \lesssim 5$ to $(r_0 m_{ps})^2 \lesssim 4$ or 6 or ∞ , i.e. include all the data. (We can go no lower than $(r_0 m_{ps})^2 \lesssim 4$ if we wish to have at least two sea quark masses in the fit for each β .) There was little change in the fit result and we shall take these changes as a systematic error, see below and section 6.2. Using $(r_0 m_{ps})^2 \lesssim 5$ means that our pseudoscalar masses range from about 440 MeV to about double that value.

As a second check on the validity of these results, let us relate them to the LECs in eqs. (26), (27) and (28) (in the continuum limit). From Table 5 and eq. (28) we find that

$$2\alpha_6 - \alpha_4 \approx -0.21, \quad 2\alpha_8 - \alpha_5 \approx -1.19. \quad (59)$$

These numbers are to be compared with the results of eq. (21) namely ≈ -0.24

$r_0 \tilde{m}_q / (r_0 m_{ps})^2$ against $(r_0 m_{ps})^2$ using $(r_0/a)_c$ which is the chirally extrapolated r_0/a would give larger NLO corrections.

and ≈ -1.02 respectively. Furthermore we have from eqs. (18), (19), (22) and (57) the relations

$$c_\chi = \frac{2B_0^{RCI}}{(4\pi f_0)^2 r_0}, \quad c_m = \frac{1}{4\pi f_0 r_0}, \quad (60)$$

where $B_0^{RCI} = [\Delta Z_m^S(M)]^{-1} B_0^S$, which give

$$B_0^{RCI} = \frac{1}{2r_0 c_a^{RCI}}. \quad (61)$$

Together with eq. (20) (using $f_0 \approx f_\pi$) and $[\Delta Z_m^{\overline{MS}}(2 \text{ GeV})]^{-1}$ from Table 1 this leads to (cf eq. (21)),

$$\langle \bar{q}q \rangle^{\overline{MS}}(2 \text{ GeV}) = - \begin{cases} (263(5)(5)(5) \text{ MeV})^3 & \text{for } r_0 = 0.5 \text{ fm} \\ (267(5)(5)(5) \text{ MeV})^3 & \text{for } r_0 = 0.467 \text{ fm} \end{cases}, \quad (62)$$

where as discussed in section 2, we consider two scales $r_0 = 0.5 \text{ fm}$ and $r_0 = 0.467 \text{ fm}$. The first error is statistical and the second is systematic $\approx 5 \text{ MeV}$ determined by the change in c_a^{RCI} when changing the fit interval, as discussed above. The third (systematic) error is due to the choice of r_0 scale, taken here as the difference between the results and also $\approx 5 \text{ MeV}$.

We find it encouraging that the c_a^{RCI} and c_i^{RCI} ($i = b, c, d$) results from the fit give numbers in rough agreement with phenomenological expectations for $2\alpha_6 - \alpha_4$, $2\alpha_8 - \alpha_5$ and the chiral condensate (and also with other lattice determinations of the chiral condensate, e.g. [49, 54]). However to obtain more accurate results will require much more precise numerical data¹².

6.2 The quark masses

We now turn to the evaluation of the strange (and light) quark masses. After finding the coefficients c_a^{RCI} , c_i^{RCI} ($i = b, c, d$), these can be substituted into eq. (29) to give for the strange quark mass

$$\begin{aligned} r_0 m_s^{RCI} &= c_a^{RCI} \left[(r_0 m_{K^+})^2 + (r_0 m_{K^0})^2 - (r_0 m_{\pi^+})^2 \right] \\ &+ (c_b^{RCI} - c_d^{RCI}) \left[(r_0 m_{K^+})^2 + (r_0 m_{K^0})^2 \right] (r_0 m_{\pi^+})^2 \\ &+ \frac{1}{2} (c_c^{RCI} + c_d^{RCI}) \left[(r_0 m_{K^+})^2 + (r_0 m_{K^0})^2 \right]^2 \\ &- (c_b^{RCI} + c_c^{RCI}) (r_0 m_{\pi^+})^4 \\ &- c_d^{RCI} \left[(r_0 m_{K^+})^2 + (r_0 m_{K^0})^2 \right] \left[(r_0 m_{K^+})^2 + (r_0 m_{K^0})^2 - (r_0 m_{\pi^+})^2 \right] \\ &\quad \times \ln \left((r_0 m_{K^+})^2 + (r_0 m_{K^0})^2 - (r_0 m_{\pi^+})^2 \right) \\ &+ c_d^{RCI} (r_0 m_{\pi^+})^4 \ln (r_0 m_{\pi^+})^2. \end{aligned} \quad (63)$$

¹²It is possible to obtain expressions and hence in principle results for f_0 , $\langle \bar{q}q \rangle$, $2\alpha_6 - \alpha_4$ and $2\alpha_8 - \alpha_5$ in terms of c_a^{RCI} and c_i^{RCI} ($i = b, c, d$). However these then all depend on the less well determined NLO c_i^{RCI} ($i = b, c, d$).

Similarly for the light quark mass we have

$$r_0 m_{ud}^{RGI} = c_a^{RGI} (r_0 m_{\pi^+})^2 + (c_b^{RGI} + c_c^{RGI}) (r_0 m_{\pi^+})^4 - c_d^{RGI} (r_0 m_{\pi^+})^4 \ln(r_0 m_{\pi^+})^2. \quad (64)$$

We first consider the strange quark mass. As can be seen from Table 5 or Fig. 11, the errors of the NLO parameters, i.e. c_i^{RGI} ($i = b, c, d$) are the same size as the signal itself and thus using them directly in eq. (63) simply gives a change in the LO result (i.e. using only the c_a^{RGI} term) of a few percent, together with a similar increase in the error (especially using error propagation; note that the third and fifth terms in eq. (63) give the main contribution to the NLO term).

To reduce the total error on the result, it proved advantageous to use eq. (63) to eliminate c_a^{RGI} from eq. (58) in terms of

$$c_{a'}^{RGI} \equiv \frac{r_0 m_s^{RGI}}{(r_0 m_{K^+})^2 + (r_0 m_{K^0})^2 - (r_0 m_{\pi^+})^2}. \quad (65)$$

This results in a modified fit function of the form

$$\begin{aligned} \frac{r_0 m_q^{RGI}}{(r_0 m_{ps})^2} = c_{a'}^{RGI} &+ c_b^{RGI} [(r_0 m_{ps}^S)^2 - d_b] + c_c^{RGI} [(r_0 m_{ps})^2 - d_c] \\ &+ c_d^{RGI} \left[\left((r_0 m_{ps}^S)^2 - 2(r_0 m_{ps})^2 \right) \ln(r_0 m_{ps})^2 - d_d \right], \end{aligned} \quad (66)$$

where d_i ($i = b, c, d$) can be read-off from eq. (63) and have the effect of shifting the various terms in the fit function by a constant. For example, the simplest to evaluate, d_b , is given by $(r_0 m_{\pi^+})^2$. Note that the fit coefficients c_i^{RGI} ($i = b, c, d$) are unchanged from those given in Table 5. Also the numerical values of the fit function are unchanged and are given by the curves in Figs. 7, 8, 9 and 10.

Note that, although we now have to choose the scale before we make the fit, the advantage is that the error on $c_{a'}^{RGI}$ gives directly the error on the strange quark mass up to NLO. Given this, it is no longer a disadvantage to consider the continuum extrapolation for $m_s^{\overline{MS}}(2 \text{ GeV})$ directly.

As discussed earlier, we shall consider two r_0 scales. Given $[\Delta Z_m^{\overline{MS}}(2 \text{ GeV})]^{-1}$ from Table 1 and using the experimental values of the π and K masses, eq. (32) to determine the ‘pure’ QCD pseudoscalar masses in eq. (31), we find the results in Table 6.

A continuum extrapolation (using $r_0 = 0.5 \text{ fm}$) is shown in Fig. 12 together with a comparison with our previous VWI results [11]. The two methods have different $O(a^2)$ discretisation errors, but should agree in the continuum. For the VWI method an extrapolation gave results of 126(5)(8) MeV, 119(5)(8) MeV for $r_0 = 0.5 \text{ fm}$ and 0.467 fm respectively. Consistent agreement between the AWI and VWI methods within error bars is found. Finally we quote our result for the strange quark mass

$$m_s^{\overline{MS}}(2 \text{ GeV}) = \begin{cases} 117(6)(4)(6) \text{ MeV} & \text{for } r_0 = 0.5 \text{ fm} \\ 111(6)(4)(6) \text{ MeV} & \text{for } r_0 = 0.467 \text{ fm} \end{cases}, \quad (67)$$

β	c_a^{RCI}		$m_s^{\overline{MS}}(2 \text{ GeV})$	
	$r_0 = 0.5 \text{ fm}$	$r_0 = 0.467 \text{ fm}$	$r_0 = 0.5 \text{ fm}$	$r_0 = 0.467 \text{ fm}$
5.20	0.1179(21)	0.1175(21)	98.71(2.33)	93.35(2.29)
5.25	0.1233(20)	0.1231(20)	103.27(2.33)	97.77(2.30)
5.29	0.1216(20)	0.1214(21)	101.79(2.33)	96.41(2.31)
5.40	0.1282(18)	0.1281(18)	107.32(2.26)	101.73(2.25)
∞	0.1393(46)	0.1395(46)	116.5(5.6)	110.7(5.5)

Table 6: Values of c_a^{RCI} and $m_s^{\overline{MS}}(2 \text{ GeV})$ together with their extrapolated (continuum) values ($\beta = \infty$). c_i^{RCI} ($i = b, c, d$) are given in Table 5.

where the first error is statistical and the second is systematic $\approx 4 \text{ MeV}$. As discussed in section 6.1, we have determined it from the effect on c_a^{RCI} of changing the fit interval. Furthermore the additional third (systematic) error due to the r_0 scale uncertainty is $\approx 6 \text{ MeV}$, see section 2.

As discussed earlier, from the values of the c_a^{RCI} , c_i^{RCI} ($i = b, c, d$) coefficients we know that the corrections due to the NLO terms are small. Using the continuum value of c_a^{RCI} from Table 5 gives for the LO strange quark mass $m_s^{\overline{MS}}(2 \text{ GeV}) = 111(6) \text{ MeV}$ and $106(6) \text{ MeV}$ for $r_0 = 0.5 \text{ fm}$, $r_0 = 0.467 \text{ fm}$ respectively. The difference is about 6 MeV , which means that NLO terms give about a 5% correction. We have not tried here to estimate the effects of higher order terms in χPT , [24].

For the light quark mass, the numerical situation is more fortunate. From Table 5, we see that $|((r_0 m_{\pi^+})^2 (c_b^{RCI} + c_c^{RCI}) / c_a^{RCI})| \approx 0.004$ and similarly for $|((r_0 m_{\pi^+})^2 \ln(r_0 m_{\pi^+})^2 c_d^{RCI} / c_a^{RCI})| \approx 0.005$, so corrections from LO to NLO χPT are at the $\frac{1}{2}\%$ level and are negligible here. We shall just quote the LO result of

$$m_{ud}^{\overline{MS}}(2 \text{ GeV}) = \begin{cases} 4.30(25)(19)(23) \text{ MeV} & \text{for } r_0 = 0.5 \text{ fm} \\ 4.08(23)(19)(23) \text{ MeV} & \text{for } r_0 = 0.467 \text{ fm} \end{cases}, \quad (68)$$

where again the second error is systematic. The third (systematic) error is due to the scale $\approx 0.23 \text{ MeV}$.

Finally, because the NLO corrections of χPT are small, we see that the ratio

$$\frac{m_s^{\overline{MS}}(2 \text{ GeV})}{m_{ud}^{\overline{MS}}(2 \text{ GeV})} = 27.2(3.2), \quad (69)$$

is close to the LO result, eq. (33).

7 Comparisons and Conclusions

In this article we have estimated the strange quark mass for two flavour QCD and found the result in eq. (67), using $O(a)$ improved clover fermions and taking into

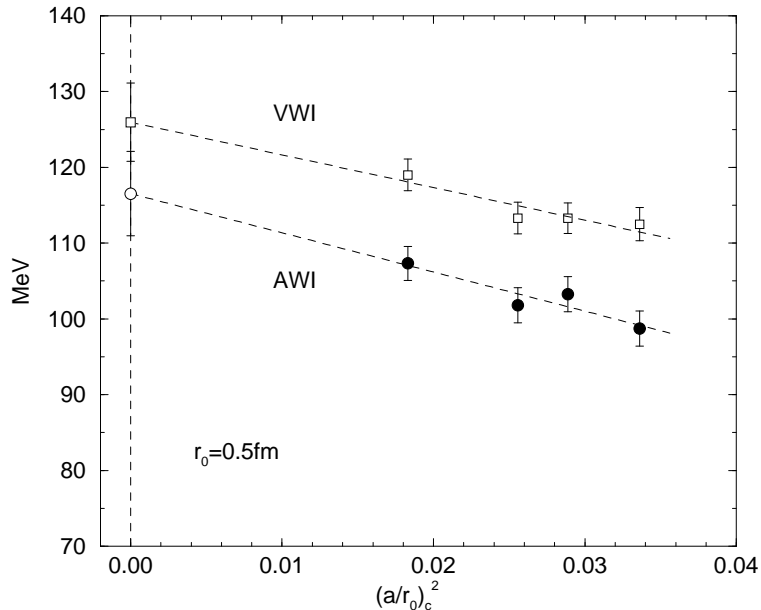


Figure 12: $m_s^{\overline{MS}}(2\text{ GeV})$ versus $(a/r_0)_c^2$ (filled circles), together with a linear continuum extrapolation (empty circle). The scale used is $r_0 = 0.5\text{ fm}$. For comparison we also show the results from using the VWI, open squares, [11].

consideration non-perturbative (NP) renormalisation, the continuum extrapolation of the lattice results and the use of chiral perturbation theory. The NLO chiral perturbation theory yields a correction of about 5% to the LO result, and the relevant low energy constants are in rough agreement with the phenomenological values.

It is also useful to compare our results with the results from other groups. In Fig. 13 we show some results for $n_f = 2$ and $n_f = 2 + 1$ flavours (keeping the aspect ratio approximately the same as in Fig. 12). A variety of actions, renormalisations, units and scales have been used (so the results have been plotted in physical units using the authors' preferred values). In particular the HPQCD-MILC-UKQCD [8] and HPQCD [6] collaborations use improved staggered fermions. These fermions having a (remnant) chiral symmetry and are in the same situation as overlap/domain wall fermions where there is no distinction between VWI and AWI quark masses; the bare quark mass in the Lagrangian simply needs to be renormalised.

As seen earlier in section 5.3 it is noticeable that the (tadpole improved) perturbative results lie lower than the non-perturbatively renormalised results. Also results with $a \lesssim 0.09\text{ fm}$ (i.e. $a^2 \lesssim 0.008\text{ fm}^2$) appear to be reasonably consistent with each other (this is more pronounced for the AWI results than for the VWI results). While results for $a \lesssim 0.09$ show some lattice discretisation effects, using results at larger lattice spacings seems to give a fairly constant extrapolation to

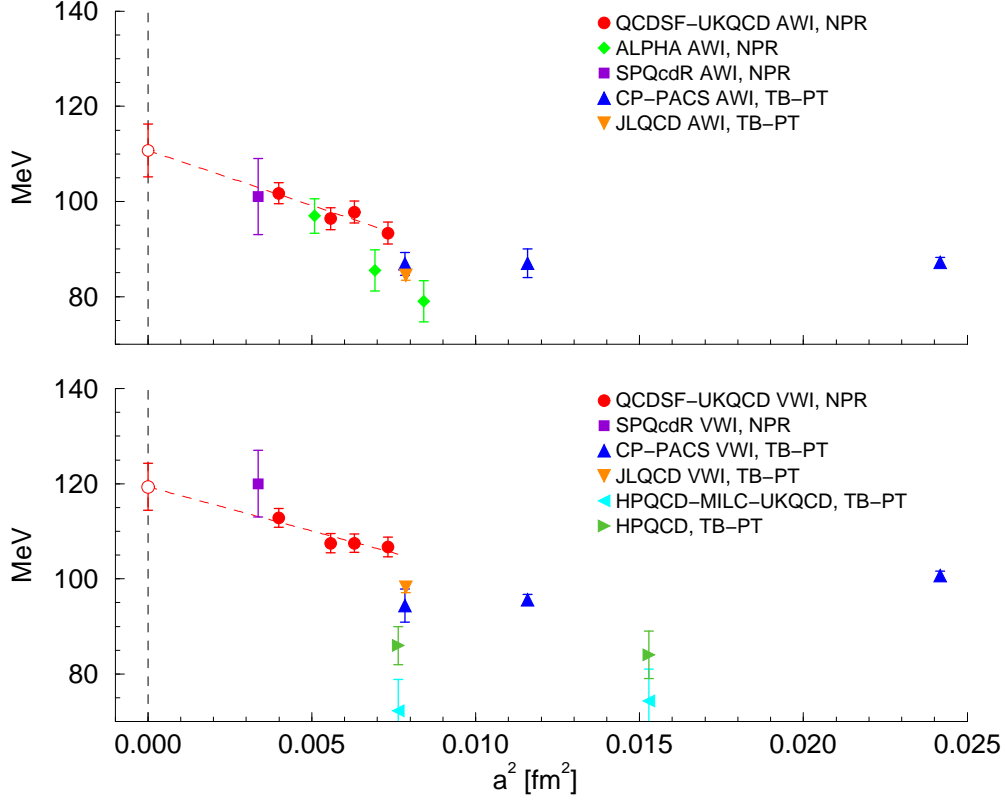


Figure 13: Results for $m_s^{\overline{MS}}(2\text{ GeV})$ versus a^2 using the AWI (upper plot) and VWI (lower plot) methods. The results are presented with the collaborations preferred units and scales. Circles (together with a linear continuum extrapolation) are from this work and [11]; diamonds from [12]; squares from [13]; up triangles from [3]; down triangles from [4]; left triangles from [6]; right triangles from [8]. NPR denotes non-perturbative renormalisation, while TB-PT denotes TI boosted perturbation theory. [6, 8] are for $n_f = 2 + 1$ flavours; the other results are all for $n_f = 2$ flavours.

the continuum limit. A similar effect has also been seen elsewhere, for example in the determination of $r_0\Lambda^{\overline{MS}}$ for $n_f = 0$ flavours, [19], where coarse lattices also show this characteristic flattening of the data.

Finally, we compare these numbers with results from the QCD sum rule approach. A review of results from this method is given in [55], citing as a final result $m_s^{\overline{MS}}(2\text{ GeV}) = 99(28)\text{ MeV}$, while a recent five-loop calculation, [56] gives $m_s^{\overline{MS}}(2\text{ GeV}) = 105(6)(7)\text{ MeV}$. These numbers cover the lattice results in Fig. 13.

In conclusion, although there is a spread of results, it would seem that the unquenched strange quark mass determined here is not lighter than the quenched strange quark mass and lies in the range of 100 – 130 MeV.

Acknowledgements

The numerical calculations have been performed on the Hitachi SR8000 at LRZ (Munich), on the Cray T3E at EPCC (Edinburgh) [58], on the Cray T3E at NIC (Jülich) and ZIB (Berlin), as well as on the APE1000 and Quadrics at DESY (Zeuthen). We thank all institutions. This work has been supported in part by the EU Integrated Infrastructure Initiative Hadron Physics (I3HP) under contract RII3-CT-2004-506078 and by the DFG under contract FOR 465 (Forschergruppe Gitter-Hadronen-Phänomenologie).

Appendix

We collect here in Tables 7, 8, 9 and 10 the numerical values of the partially quenched am_{ps} and the bare AWI quark terms $a\widetilde{m}_q^{(0)}$, $a\widetilde{m}_q^{(1)}$ and $a\widetilde{m}_q$. These are defined in eq. (39) as ratios of certain correlation functions. (The operators are summed over spatial planes, the time derivatives being taken as in footnotes 4 and 6.) The (bootstrap) errors for the ratios are given uniformly to two significant figures, with the overriding requirement that the result must also have a minimum of four significant figures.

The second column in the tables gives the pion mass, defined in the standard way from the correlation function

$$\langle P^{smearred}(t)P^{smearred}(0) \rangle \stackrel{t \gg 0}{\cong} A \left(e^{-m_{ps}t} + e^{-m_{ps}(aN_T-t)} \right), \quad (70)$$

where the correlation function is evaluated in a configuration with sea quark mass am_q^S . (The normalisation is not important here so we can work with unimproved operators to obtain the pseudoscalar masses.) The smearing used is Jacobi smearing (see e.g. [57]), with typical parameters $\kappa_s = 0.21$ and $n_s = 50$.

The third and fourth columns in the tables give the bare results for $a\widetilde{m}_q^{(0)}$ and $a\widetilde{m}_q^{(1)}$, as defined in eq. (39).

The improvement coefficient c_A has been determined non-perturbatively in [20]. We use the values obtained there of

β	c_A
5.20	-0.0641(40)
5.25	-0.0565(40)
5.29	-0.0517(40)
5.40	-0.0420(40)

(71)

From the tables it can be seen that the inclusion of the improvement term ($\times c_A$) to the quark mass gives a noticeable change in the final result. Also the error in c_A has an effect. Although not a large difference to using simple error propagation for the three quantities ($a\widetilde{m}_q^{(0)}$, $a\widetilde{m}_q^{(1)}$ and c_A), to try to minimize the error propagation we have adopted the procedure of first finding the bootstrap error for $a\widetilde{m}_q^{(0)} + c_A a\widetilde{m}_q^{(1)}$ (with fixed c_A) and then including the independent error of c_A (\times fixed $a\widetilde{m}_q^{(1)}$) by error propagation. This gives the results for $a\widetilde{m}_q$ shown in the fifth column of the tables.

κ_q	am_{ps}	$a\tilde{m}_q^{(0)}$	$a\tilde{m}_q^{(1)}$	$a\tilde{m}_q$
$\kappa_q^S = 0.1342$				
0.1334	0.6581(12)	0.11221(19)	0.22501(73)	0.09778(16)
0.1338	0.6224(12)	0.10010(19)	0.20041(70)	0.08724(16)
0.1342	0.5847(12)	0.08821(19)	0.17647(67)	0.07689(16)
0.1347	0.5359(12)	0.07366(19)	0.14744(63)	0.06420(16)
0.1353	0.4720(13)	0.05664(19)	0.11383(60)	0.04934(16)
0.1356	0.4371(14)	0.04828(19)	0.09743(59)	0.04203(16)
0.1360	0.3856(16)	0.03715(22)	0.07576(60)	0.03229(19)
0.1362	0.3569(17)	0.03159(25)	0.06515(64)	0.02741(22)
$\kappa_q^S = 0.1350$				
0.1332	0.5985(11)	0.10076(16)	0.18529(60)	0.08888(13)
0.1337	0.5515(11)	0.08566(16)	0.15670(58)	0.07561(13)
0.1342	0.5018(11)	0.07088(15)	0.12923(55)	0.06260(13)
0.1345	0.4703(12)	0.06218(15)	0.11327(54)	0.05492(13)
0.1350	0.4148(13)	0.04785(15)	0.08755(54)	0.04224(13)
0.1353	0.3771(15)	0.03954(17)	0.07246(54)	0.03490(14)
0.1355	0.3505(19)	0.03397(18)	0.06256(57)	0.02996(16)
0.1357	0.3216(20)	0.02837(20)	0.05293(57)	0.02497(17)
$\kappa_q^S = 0.1355$				
0.1332	0.5546(10)	0.09121(14)	0.15890(54)	0.08102(12)
0.1336	0.5158(11)	0.07911(14)	0.13707(52)	0.07032(13)
0.1340	0.4751(11)	0.06718(15)	0.11600(51)	0.05974(13)
0.1343	0.4430(12)	0.05842(15)	0.10069(50)	0.05196(13)
0.1348	0.3848(14)	0.04410(15)	0.07610(51)	0.03922(14)
0.1350	0.3600(15)	0.03847(15)	0.06656(51)	0.03421(14)
0.1353	0.3200(17)	0.03014(16)	0.05252(53)	0.02677(14)
0.1355	0.2907(15)	0.02451(15)	0.04275(43)	0.02177(13)
0.1357	0.2577(23)	0.01909(18)	0.03475(51)	0.01687(16)

Table 7: The bare results for am_{ps} , $a\tilde{m}_q^{(0)}$, $a\tilde{m}_q^{(1)}$ and $a\tilde{m}_q$ for $\beta = 5.20$.

κ_q	am_{ps}	$a\widetilde{m}_q^{(0)}$	$a\widetilde{m}_q^{(1)}$	$a\widetilde{m}_q$
$\kappa_q^S = 0.1346$				
0.1337	0.5794(15)	0.09697(19)	0.17225(87)	0.08723(17)
0.1340	0.5514(15)	0.08793(19)	0.15554(86)	0.07914(17)
0.1346	0.4932(10)	0.07027(12)	0.12399(47)	0.06326(11)
0.1349	0.4612(17)	0.06148(18)	0.10782(79)	0.05539(17)
0.1353	0.4168(18)	0.05005(18)	0.08774(76)	0.04509(17)
0.1355	0.3932(18)	0.04440(18)	0.07794(75)	0.03999(17)
0.1359	0.3420(20)	0.03317(19)	0.05877(64)	0.02985(18)
0.1361	0.3133(22)	0.02750(21)	0.04913(65)	0.02472(19)
$\kappa_q^S = 0.1352$				
0.1337	0.5419(11)	0.08860(16)	0.15186(60)	0.08002(14)
0.1341	0.5027(12)	0.07658(16)	0.13073(57)	0.06919(14)
0.1345	0.4621(13)	0.06474(16)	0.11027(54)	0.05851(14)
0.1348	0.4300(13)	0.05599(16)	0.09536(52)	0.05060(14)
0.1352	0.3821(13)	0.04432(12)	0.07471(38)	0.04010(10)
0.1355	0.3466(17)	0.03593(17)	0.06178(50)	0.03244(16)
0.1358	0.3054(20)	0.02740(19)	0.04775(53)	0.02470(18)
0.1359	0.2901(22)	0.02452(21)	0.04309(56)	0.02209(20)
$\kappa_q^S = 0.13575$				
0.1336	0.50970(72)	0.084021(81)	0.13257(36)	0.076528(72)
0.1339	0.48011(72)	0.074990(81)	0.11733(35)	0.068359(72)
0.1343	0.43883(73)	0.063110(80)	0.09772(33)	0.057587(73)
0.1346	0.40619(74)	0.054323(81)	0.08354(31)	0.049601(74)
0.1350	0.35966(76)	0.042776(83)	0.06532(28)	0.039085(76)
0.1352	0.33469(77)	0.037071(84)	0.05657(24)	0.033874(78)
0.1355	0.29421(81)	0.028608(87)	0.04360(22)	0.026144(81)
0.13575	0.25556(55)	0.021495(57)	0.03291(15)	0.019635(52)
0.1360	0.2117(13)	0.01456(11)	0.02256(26)	0.013281(98)

Table 8: The bare results for am_{ps} , $a\widetilde{m}_q^{(0)}$, $a\widetilde{m}_q^{(1)}$ and $a\widetilde{m}_q$ for $\beta = 5.25$.

κ_q	am_{ps}	$a\widetilde{m}_q^{(0)}$	$a\widetilde{m}_q^{(1)}$	$a\widetilde{m}_q$
$\kappa_q^S = 0.1340$				
0.1340	0.5767(11)	0.09689(19)	0.17170(60)	0.08802(17)
0.1344	0.5392(15)	0.08480(18)	0.14841(82)	0.07713(16)
0.1349	0.4901(16)	0.07010(18)	0.12204(81)	0.06379(16)
0.1352	0.4589(17)	0.06141(19)	0.10669(80)	0.05590(17)
0.1355	0.4255(17)	0.05283(19)	0.09169(80)	0.04809(17)
0.1357	0.4024(20)	0.04715(19)	0.08189(80)	0.04292(17)
0.1359	0.3781(21)	0.04151(20)	0.07226(80)	0.03778(18)
0.1362	0.3384(23)	0.03315(23)	0.05830(81)	0.03013(21)
$\kappa_q^S = 0.1350$				
0.1340	0.52221(81)	0.08542(11)	0.14024(41)	0.078169(94)
0.1343	0.49323(83)	0.07643(11)	0.12483(40)	0.069978(96)
0.1347	0.45278(86)	0.06460(11)	0.10489(39)	0.059180(99)
0.1350	0.42057(92)	0.05584(11)	0.09036(34)	0.051171(95)
0.1355	0.3634(10)	0.04146(11)	0.06707(38)	0.03799(10)
0.1357	0.3381(10)	0.03577(12)	0.05794(38)	0.03277(11)
0.1360	0.2963(12)	0.02722(12)	0.04452(39)	0.02492(11)
0.1361	0.2798(17)	0.02427(15)	0.03963(54)	0.02222(13)
$\kappa_q^S = 0.1355$				
0.1339	0.49968(92)	0.08260(11)	0.12790(44)	0.075988(94)
0.1343	0.46105(86)	0.07062(10)	0.10825(41)	0.065025(93)
0.1346	0.43015(86)	0.06175(10)	0.09402(38)	0.056888(92)
0.1349	0.39774(87)	0.05297(10)	0.08023(36)	0.048825(92)
0.1353	0.35144(91)	0.04142(10)	0.06252(34)	0.038192(93)
0.1355	0.32688(70)	0.035783(77)	0.05417(22)	0.032983(71)
0.1358	0.2858(11)	0.02723(11)	0.04151(30)	0.02508(10)
0.1360	0.2552(14)	0.02159(13)	0.03316(31)	0.01988(12)
0.1363	0.2012(18)	0.01304(14)	0.02056(30)	0.01197(13)
$\kappa_q^S = 0.1359$				
0.1339	0.47757(65)	0.078462(92)	0.11620(29)	0.072456(88)
0.13425	0.44247(66)	0.067952(92)	0.09946(28)	0.062811(88)
0.1346	0.40540(70)	0.057566(92)	0.08333(27)	0.053259(88)
0.13505	0.35469(70)	0.044401(93)	0.06350(25)	0.041119(89)
0.13531	0.32287(73)	0.036894(94)	0.05251(24)	0.034180(90)
0.13562	0.28151(78)	0.028036(96)	0.03982(23)	0.025977(91)
0.1359	0.23924(87)	0.020134(92)	0.02886(21)	0.018642(86)
0.13617	0.1899(12)	0.01239(10)	0.01837(25)	0.011444(98)

Table 9: The bare results for am_{ps} , $a\widetilde{m}_q^{(0)}$, $a\widetilde{m}_q^{(1)}$ and $a\widetilde{m}_q$ for $\beta = 5.29$.

κ_q	am_{ps}	$a\tilde{m}_q^{(0)}$	$a\tilde{m}_q^{(1)}$	$a\tilde{m}_q$
$\kappa_q^S = 0.1350$				
0.1346	0.44399(52)	0.071849(57)	0.10023(25)	0.067635(52)
0.1350	0.40301(43)	0.059913(50)	0.08250(18)	0.056444(47)
0.1353	0.37156(54)	0.051132(70)	0.06996(21)	0.048190(67)
0.1357	0.32541(63)	0.039519(68)	0.05359(21)	0.037266(64)
0.13602	0.28482(69)	0.030274(70)	0.04100(21)	0.028550(66)
0.1363	0.24504(77)	0.022220(72)	0.03027(20)	0.020947(68)
0.13655	0.20349(95)	0.014975(74)	0.02098(22)	0.014093(70)
0.1366	0.1934(13)	0.013555(84)	0.01950(39)	0.012735(79)
$\kappa_q^S = 0.1356$				
0.1346	0.42009(66)	0.067720(51)	0.08973(29)	0.063947(47)
0.13494	0.38581(63)	0.057620(49)	0.07533(28)	0.054453(45)
0.1353	0.34617(72)	0.046987(49)	0.06068(26)	0.044436(46)
0.1356	0.31232(67)	0.038239(49)	0.04926(22)	0.036168(44)
0.13591	0.27210(77)	0.029197(52)	0.03725(24)	0.027631(50)
0.13618	0.23346(87)	0.021380(56)	0.02742(23)	0.020227(53)
0.13643	0.1921(10)	0.014081(68)	0.01873(22)	0.013293(65)
0.1365	0.1796(12)	0.01185(14)	0.01629(34)	0.01116(13)
$\kappa_q^S = 0.1361$				
0.1346	0.40055(60)	0.064373(49)	0.08174(23)	0.060936(45)
0.13493	0.36621(63)	0.054572(47)	0.06820(22)	0.051704(44)
0.13525	0.33068(70)	0.045072(53)	0.05559(21)	0.042735(50)
0.13555	0.29521(76)	0.036298(51)	0.04425(20)	0.034437(49)
0.13584	0.25784(85)	0.027842(55)	0.03372(20)	0.026425(53)
0.1361	0.22081(72)	0.020335(47)	0.02455(16)	0.019303(44)
0.13632	0.1833(12)	0.013937(71)	0.01705(22)	0.013220(68)
0.1364	0.1668(19)	0.011552(88)	0.01457(22)	0.010940(84)

Table 10: The bare results for am_{ps} , $a\tilde{m}_q^{(0)}$, $a\tilde{m}_q^{(1)}$ and $a\tilde{m}_q$ for $\beta = 5.40$.

References

- [1] QCDSF-UKQCD Collaboration: T. Bakeyev, M. Göckeler, R. Horsley, D. Pleiter, P. E. L. Rakow, G. Schierholz and H. Stüben, *Phys. Lett.* **B580** (2004) 197 [hep-lat/0305014].
- [2] CP-PACS Collaboration: A. Ali Khan, S. Aoki, G. Boyd, R. Burkhalter, S. Ejiri, M. Fukugita, S. Hashimoto, N. Ishizuka, Y. Iwasaki, K. Kanaya, T. Kaneko, Y. Kuramashi, T. Manke, K. Nagai, M. Okawa, H. P. Shanahan, A. Ukawa and T. Yoshié, *Phys. Rev. Lett.* **85** (2000) 4674 [Erratum-ibid. **90** (2003) 029902] [hep-lat/0004010].
- [3] CP-PACS Collaboration: A. Ali Khan, S. Aoki, G. Boyd, R. Burkhalter, S. Ejiri, M. Fukugita, S. Hashimoto, N. Ishizuka, Y. Iwasaki, K. Kanaya, T. Kaneko, Y. Kuramashi, T. Manke, K. Nagai, M. Okawa, H.P. Shanahan, A. Ukawa and T. Yoshié, *Phys. Rev.* **D65** (2002) 054505 [Erratum-ibid. **D67** (2003) 059901] [hep-lat/0105015].
- [4] JLQCD Collaboration: S.Aoki, R. Burkhalter, M. Fukugita, S. Hashimoto, K-I. Ishikawa, N. Ishizuka, Y. Iwasaki, K. Kanaya, T. Kaneko, Y. Kuramashi, M. Okawa, T. Onogi, N. Tsutsui, A. Ukawa, N. Yamada and T. Yoshié, *Phys. Rev.* **D68** (2003) 054502 [hep-lat/0212039].
- [5] CP-PACS Collaboration: T. Kaneko, S.Aoki, M. Fukugita, S. Hashimoto, K-I. Ishikawa, T. Ishikawa, N. Ishizuka, Y. Iwasaki, K. Kanaya, Y. Kuramashi, M. Okawa, N. Taniguchi, N. Tsutsui, A. Ukawa and T. Yoshié, *Nucl. Phys. Proc. Suppl.* **129** (2004) 188 [hep-lat/0309137].
- [6] HPQCD-MILC-UKQCD Collaboration: C. Aubin, C. Bernard, C. Davies, C. DeTar, S. Gottlieb, A. Gray, E. Gregory, J. Hein, U. Heller, J. Hetrick, G. P. Lepage, Q. Mason, J. Osborn, J. Shigemitsu, R. Sugar, D. Toussaint, H. Trottier and M. Wingate, *Phys. Rev.* **D70** (2004) 031504 [hep-lat/0405022].
- [7] CP-PACS–JLQCD Collaboration: T. Ishikawa, S. Aoki, O. Bär, M. Fukugita, S. Hashimoto, K.-I. Ishikawa, N. Ishizuka, Y. Iwasaki, K. Kanaya, T. Kaneko, Y. Kuramashi, M. Okawa, Y. Taniguchi, N. Tsutsui, A. Ukawa and T. Yoshié, *Proc. of Sci.* PoS(LAT2005)057 [hep-lat/0509142].
- [8] HPQCD Collaboration: Q. Mason, H. D. Trottier, R. Horgan, C. T. H. Davies, and G. P. Lepage, hep-ph/0511160.
- [9] QCDSF Collaboration: M. Göckeler, R. Horsley, H. Oelrich, D. Petters, D. Pleiter, P. E. L. Rakow, G. Schierholz and P. Stephenson, *Phys. Rev.* **D62** (2000) 054504 [hep-lat/9908005].

- [10] ALPHA-UKQCD Collaboration: J. Garden, J. Heitger, R. Sommer and H. Wittig, *Nucl. Phys.* **B571** (2000) 237 [hep-lat/9906013].
- [11] QCDSF-UKQCD Collaboration: M. Göckeler, R. Horsley, A. C. Irving, D. Pleiter, P. E. L. Rakow, G. Schierholz and H. Stüben, hep-ph/0409312.
- [12] ALPHA Collaboration: M. Della Morte, R. Hoffmann, F. Knechtli, J. Rolf, R. Sommer, I. Wetzorke and U. Wolff, *Nucl. Phys.* **B729** (2005) 117 [hep-lat/0507035].
- [13] SPQcdR Collaboration: D. Bećirević, B. Blossier, P. Boucaud, V. Giménez, V. Lubicz, F. Mescia, S. Simula and C. Tarantino, hep-lat/0510014.
- [14] O. V. Tarasov, A. A. Vladimirov and A. Yu. Zharkov, *Phys. Lett.* **B93** (1980) 429.
- [15] S. A. Larin and J. A. M. Vermaseren, *Phys. Lett.* **B303** (1993) 334, [hep-ph/9302208].
- [16] T. van Ritbergen, J. A. M. Vermaseren and S. A. Larin, *Phys. Lett.* **B400** (1997) 379 [hep-ph/9701390].
- [17] K. G. Chetyrkin, *Phys. Lett.* **B404** (1997) 161 [hep-ph/9703278].
- [18] J. A. M. Vermaseren, S. A. Larin and T. van Ritbergen, *Phys. Lett.* **B405** (1997) 327 [hep-ph/9703284].
- [19] QCDSF-UKQCD Collaboration: M. Göckeler, R. Horsley, A. C. Irving, D. Pleiter, P. E. L. Rakow, G. Schierholz and H. Stüben, to be published in *Phys. Rev.* **D** [hep-ph/0502212].
- [20] ALPHA Collaboration: M. Della Morte, R. Frezzotti, J. Heitger, J. Rolf, R. Sommer and U. Wolff, *Nucl. Phys.* **B713** (2005) 378 [hep-lat/0411025].
- [21] QCDSF-UKQCD Collaboration: A. Ali Khan, T. Bakeyev, M. Göckeler, T. R. Hemmert, R. Horsley, A. C. Irving, B. Joó, D. Pleiter, P. E. L. Rakow, G. Schierholz and H. Stüben, *Nucl. Phys.* **B689** (2004) 175 [hep-lat/0312030].
- [22] C. Aubin, C. Bernard, C. DeTar, S. Gottlieb, E. B. Gregory, U. M. Heller, J. E. Hetrick, J. Osborn, R. Sugar and D. Toussaint, *Phys. Rev.* **D70** (2004) 094505 [hep-lat/0402030].
- [23] QCDSF-UKQCD Collaboration: M. Göckeler, R. Horsley, D. Pleiter, P. E. L. Rakow, G. Schierholz, W. Schroers, H. Stüben and J. M. Zanotti, *Proc. of Sci* PoS(LAT2005)063 [hep-lat/0509196].
- [24] J. Bijnens and T. A. Lähde, *Phys. Rev.* **D72** (2005) 074502 [hep-lat/0506004].

- [25] C. Bernard and M. Golterman, *Phys. Rev.* D49 (1994) 486 [hep-lat/9306005].
- [26] S. R. Sharpe, *Phys. Rev.* D56 (1997) 7052, erratum ibid. D62 (2000) 099901 [hep-lat/9707018].
- [27] J. Heitger, R. Sommer and H. Wittig, *Nucl. Phys.* B588 (2000) 377 [hep-lat/0006026].
- [28] M. Jamin, *Phys. Lett.* B538 (2002) 71 [hep-ph/0201174].
- [29] T-P. Cheng and L-F. Li, Gauge Theory of elementary particle physics, Oxford University Press (1984).
- [30] H. Leutwyler, *Nucl. Phys. Proc. Suppl.* 94 (2001) 108 [hep-ph/0011049]
- [31] J. Bijnens, *Phys. Lett.* B306 (1993) 343 [hep-ph/9302217].
- [32] R. Baur and R. Urech, *Phys. Rev.* D53 (1996) 6552 [hep-ph/9508393].
- [33] H. Leutwyler, *Phys. Lett.* B378 (1996) 313 [hep-ph/9602366].
- [34] Y. Namekawa and Y. Kikukawa, *Proc. of Sci.* PoS(LAT2005)090 [hep-lat/0509120].
- [35] RBC Collaboration: N. Yamada, T. Blum, M. Hayakawa and T. Izubuchi, *Proc. of Sci.* PoS(LAT2005)092 [hep-lat/0509124].
- [36] M. Della Morte, R. Hoffmann and R. Sommer, *JHEP* 0503 (2005) 029 [hep-lat/0503003].
- [37] S. Sint and P. Weisz, *Nucl. Phys.* B502 (1997) 251 [hep-lat/9704001].
- [38] ALPHA Collaboration: M. Guagnelli, R. Petronzio, J. Rolf, S. Sint, R. Sommer and U. Wolff, *Nucl. Phys.* B595 (2001) 44 [hep-lat/0009021].
- [39] QCDSF Collaboration: M. Göckeler, R. Horsley, D. Pleiter, P. E. L. Rakow, A. Schäfer, G. Schierholz, H. Stüben and J. M. Zanotti, *Phys. Rev.* D72 (2005) 054507 [hep-lat/0506017].
- [40] QCDSF Collaboration: M. Göckeler, R. Horsley, D. Pleiter, P. E. L. Rakow and G. Schierholz, *Phys. Rev.* D71 (2005) 114511 [hep-ph/0410187].
- [41] G. Martinelli, C. Pittori, C. T. Sachrajda, M. Testa and A. Vladikas, *Nucl. Phys.* B445 (1995) 81 [hep-lat/9411010].
- [42] QCDSF Collaboration: M. Göckeler, R. Horsley, H. Oelrich, H. Perlt, D. Petters, P. E. L. Rakow, A. Schäfer, G. Schierholz and A. Schiller, *Nucl. Phys.* B544 (1999) 699 [hep-lat/9807044].

- [43] E. Franco and V. Lubicz, *Nucl. Phys.* **B531** (1998) 641 [hep-ph/9803491].
- [44] K. G. Chetyrkin and A. Rétey, *Nucl. Phys.* **B583** (2000) 3 [hep-ph/9910332].
- [45] K. G. Chetyrkin and A. Rétey, hep-ph/0007088.
- [46] J. R. Cudell, A. Le Yaouanc and C. Pittori, *Phys. Lett.* **B454** (1999) 105 [hep-lat/9810058].
- [47] K. D. Lane, *Phys. Rev.* **D10** (1974) 2605.
- [48] H. Pagels, *Phys. Rev.* **D19** (1979) 3080.
- [49] D. Bécirević and V. Lubicz *Phys. Lett.* **B600** (2004) 83 [hep-ph/0403044].
- [50] L. Giusti and A. Vladikas, *Phys. Lett.* **B488** (2000) 303 [hep-lat/0005026].
- [51] QCDSF Collaboration: S. Capitani, M. Göckeler, R. Horsley, D. Pleiter, P. Rakow, H. Stüben and G. Schierholz, *Nucl. Phys. Proc. Suppl.* **106** (2002) 299 [hep-lat/0111012].
- [52] QCDSF Collaboration: S. Capitani, M. Göckeler, R. Horsley, H. Perlt, P. E. L. Rakow, G. Schierholz and A. Schiller, *Nucl. Phys.* **B593** (2001) 183 [hep-lat/0007004].
- [53] ALPHA collaboration: M. Della Morte, R. Hoffmann, F. Knechtli, R. Sommer and U. Wolff, *JHEP* **0507** (2005) 007 [hep-lat/0505026].
- [54] C. McNeile, *Phys. Lett.* **B619** (2005) 124 [hep-lat/0504006].
- [55] S. Narison, hep-ph/0510108.
- [56] K. G. Chetyrkin and A. Khodjamirian, hep-ph/0512295.
- [57] QCDSF Collaboration: C. Best, M. Göckeler, R. Horsley, E.-M. Ilgenfritz, H. Perlt, P. Rakow, A. Schäfer, G. Schierholz, A. Schiller and S. Schramm, *Phys. Rev.* **D56** (1997) 2743 [hep-lat/9703014].
- [58] UKQCD Collaboration: C. R. Allton, S. P. Booth, K. C. Bowler, J. Garden, A. Hart, D. Hepburn, A. C. Irving, B. Joó, R. D. Kenway, C. M. Maynard, C. McNeile, C. Michael, S. M. Pickles, J. C. Sexton, K. J. Sharkey, Z. Sroczynski, M. Talevi, M. Teper and H. Wittig, *Phys. Rev.* **D65** (2002) 054502 [hep-lat/0107021].